FunGlass School 2018/part 2

Book of Abstracts

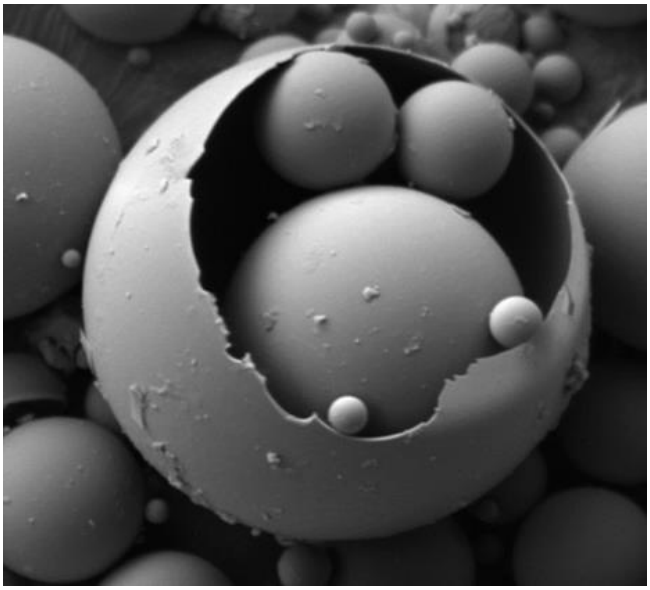

Trenčianske Teplice, November 28-30, 2018

ORGANIZING INSTITUTIONS:

FunGlass School 2018 / part 2

Book of Abstracts

Trenčianske Teplice, November 28- 30, 2018

SCIENTIFIC BOARD: Dušan Galusek, Prof., DSc., Marek Liška, Prof., DSc.

REVIEWERS: Alfonz Plško, Assoc. Prof., Martin Michálek, PhD., Jozef Kraxner, PhD., Robert Klement, PhD.

Edited by Mgr. Vanda Mokráňová

ISBN 978-80-8075-835-6
EAN 9788080758356

This conference is part of a project that has received funding from the **European Union's Horizon 2020 research and innovation programme under grant agreement №739566**

FunGlass
centre for functional and surface functionalized glass

O B S A H

M.Liška / Parameterization of thermodynamic models 3

R. Klement / Photoluminescence properties of Ce^{3+}-doped and $Ce^{3+}/Mn^{2+/4+}$ co-doped $Y_3Al_5O_{12}$ phosphors obtained by crystallization of yttrium aluminate glass with eutectic composition 5

A. Prnová / HP sintering of yttrium-aluminate glass microspheres 7

P. Švančárek / Sintering experiments and luminescent properties of Zn2+ doped Y2O3 9

A. Plško / Functionalization of glass by sol-gel layers 12

Nibu, P. G. / Yttria nanopowders for transparent yttria ceramics prepared by precipitation sol-gel method 13

F. Dogrul / Effects of test parameters on the production of hexagonal boron nitride by dcrn method 15

N. Kamble / An overview: Polymer Derived Ceramic (PDC) Coating on stainless steel 18

M. Parchovianský / Preparation, investigation and characterization of polysilazane-derived (oxy)nitride coatings on steel substrate 20

J. Vráblová / Effect of Gamma Radiation on the Chemical Durability of Glass Fibrous Insulation Used in Nuclear Power Plants 22

J. Michálková / Structure and properties of glass fibers insulation used in nuclear power plants 24

B. Hruška / Raman spectroscopy and PCA, MCR study of heavy weathered glass 25

P. Chrást / Novel borophosphosilicate bioactive glass composition – analysis and corrosion behavior 27

F. Kurtuldu / Mesoporous Bioactive Glass – Part 1: Processing and Application 30

Z. Neščáková / Mesoporous bioactive glasses – Part II: Biological response 32

S. Sengupta / A traditional technique for obtaining 3D bioactive glass scaffolds with bone like structure 34

N. Mutlu / Incorporation of Fibrous/Particulate Bioglass in Soft Matrices for Soft Tissue Applications 36

D. Galusková, H. Kaňková / Inline measurement of leachates from bioglass immersion tests 38

J. Valúchová / Flame synthesis of binary aluminate glass microspheres 40

K. Faturíková / The temperature dependence of the impedance spectrum of the barium crystal glass 41

P. Šimon / Some Peculiarities of the Isoconversional Methods 42

Parameterization of thermodynamic models

M. Liška*[1], M. Chromčíková[1], J. Macháček[2]

[1] FunGlass – Vitrum Laugaricio – Joint Glass Center of IIC SAS, TnU AD, and FChPT STU
Študentská 2, Trenčín, SK – 911 50, Slovak Republic
(E-mail: marek.liska@tnuni.sk, maria.chromcikova@tnuni.sk)
[2] University of Chemistry and Technology, Faculty of Chemical Technology, Technická 5, Prague, CZ – 166 28, Czech Republic (E-mail: jan.machacek@vscht.cz)

ABSTRACT

Mainly in the field of silicate glasses, the thermodynamic model of Shakhmatkin and Vedishcheva (SVTDM) was successfully applied in previous years [1, 2]. This model considers glasses and melts as an ideal solution formed from salt-like products of equilibrium chemical reactions between the simple chemical entities (oxides, halogenides, chalcogenides…) and from the original (un-reacted) entities. These salt-like products (also called associates, groupings or species) have the same stoichiometry as the crystalline compounds, which exist in the equilibrium phase diagram of the considered system. The model does not use adjustable parameters - only the molar Gibbs energies of pure crystalline compounds and the analytical composition of the system considered are used as input parameters. The minimization of the system's Gibbs energy constrained by the overall system composition has to be performed with respect to the molar amount of each system component to reach the equilibrium system composition [3]. The contemporary databases of thermodynamic properties containing the molar Gibbs energies of various species (like the FACT database [4, 5]) enable the routine construction of the Shakhmatkin and Vedishcheva models for many important multicomponent systems.

On the level of structural groupings (e.g. Q^n units) the glass structure is obtained as "weighted mixture" of structures of system components considered in SVTDM. However, in some cases there is missing the stable crystalline compound corresponding to the particular structural grouping. In this case some hypothetical system component is added to the model and the molar Gibbs energy of this component is obtained by minimizing the sum of squares of deviations between the calculated and experimental glass structure represented by relative amounts of different Q units [2]. However, starting rough estimates of unknown molar Gibbs energies are needed for such regression treatment. The typical example is $CaO\text{-}SiO_2$ system, where the representative of the Q^3 unit, i.e. the calcium disilicate $CaO{\cdot}2SiO_2$ (CS2), is not present in the equilibrium phase diagram [6]. On the other hand, the significant abundance of Q^3 unit in $CaO\text{-}SiO_2$ glasses was found by MAS NMR and Raman spectroscopy [7, 8].

Table I. Characteristics of $CaO\text{-}SiO_2$ SVTDM components (T = 1000 K).

Component	**Abbrev.**	**Q^n**	***NBO***	**$-G_m$ /** kJ/mol	**$-\Delta_r G_m$ /** kJ/mol	**$-\Delta_r G_m$ / NBO /** kJ/mol
CaO		-	-	697.08	-	
SiO_2		Q^4	0	981.44	-	
$2CaO{\cdot}SiO_2$	C2S	Q^0	4	2502.70	127.10	31.775
$3CaO{\cdot}2SiO_2$	C3S2	$2Q^1$	6	4283.40	229.28	38.213
$CaO{\cdot}SiO_2$	CS	Q^2	2	1767.10	88.58	44.290
$3CaO{\cdot}SiO_2$	C3S	Q^0	4	3187.40	114.72	28.680
$CaO{\cdot}2SiO_2$	**CS2**	**$2Q^3$**	**2**	**2761.18**	**101.22**	**50.608**

We propose a method of estimating of the CS2 molar Gibbs energy based on the linear relationship between the reaction Gibbs energies (□$_r G_m$) of formation of different Q^n units per one non-bridging oxygen (NBO) and the number of bridging oxygen atoms n of particular Q^n unit. In the Table I the SVTDM system components are summarized with their (experimental) molar Gibbs energies together with the results obtained by the proposed method for CS2. The estimated value gives the calculated Q-distribution close to the experimental

one. Moreover no significant improvement can be reached by adjusting the value of G_m(CS2) – the optimized value obtained such way (-2762.20 kJ/mol) is practically identical with the starting estimate (-2761.18 kJ/mol). Comparison of results obtained without CS2, with added CS2 with estimated G_m, and with added CS2 with optimized G_m are summarized in Fig. 1.

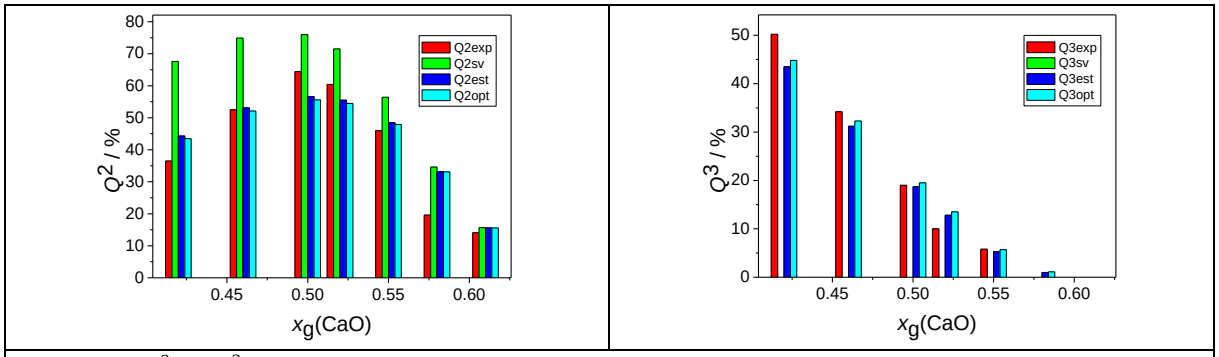

Figure 1: Q^2 & Q^3 distribution - from left: experimental, without CS2, G_m estimated, optimized.

It can be concluded that the proposed method gives the G_m estimate of very high quality. Further study of application of the proposed method to other glass forming systems is needed.

Keywords: TD model of Shakhmatkin and Vedishcheva, CaO-SiO2 glass, molar Gibbs energy

Acknowledgment:

This paper is a part of dissemination activities of project FunGlass.
This project has received funding from the European Union´s Horizon 2020 research and innovation programme under grant agreement No 739566.
The Slovak Grant Agency for Science supported this work under grants No. VEGA 2/0088/16, and VEGA 1/0064/18. This work was supported by the project of Interreg program between Slovak republic and Czech republic (2014 – 2020) „*Rozvoj vzdelávacej infraštruktúry Bielokarpatskej sklárskej základne*“, ITMS code: 304011C847.

References:

/1/ N.M. Vedishcheva, A.C. Wright, *Chemical structure of oxide glasses: A concept for establishing structure–property relationships*. In *GLASS Selected properties and crystallization.* Schmelzer J.W.P. (Editor), Chapter 5, p. 269-299, De Gruyter, Berlin 2014. ISBN 978-3-11-029838-3.

/2/ J. Macháček, M. Chromčíková, M. Liška, *Parameterization and validation of thermochemical models of glass by advanced statistical analysis of spectral data*. In *Thermal Physics and Thermal Analysis: From Macro to Micro, Highlighting Thermodynamics Kinetics and Nanomaterials*. J. Šesták, P. Hubík, J.J. Mareš (Editors), Chapter 12, p. 257-278, Springer, Switzerland 2017. ISBN 978-3-319-45897-7.

/3/ P. Voňka, J. Leitner, *Calculation of chemical equilibria in heterogeneous multicomponent systems*. Calphad. 19 (1995) 25-36.

/4/ http://www.crct.polymtl.ca/fact/, November 2018.

/5/ C.W. Bale, E. Bélisle, P.S. Chartrand, S.A. Decterov, G. Eriksson, K. Hack, I.H. Jung, Y.B. Kang, J. Melançon, A.D. Pelton, C. Robelin, S. Petersen. *FactSage Thermochemical Software and Databases – Recent Developments*. Calphad. 33 (2009) 295-311.

/6/ ACerS-NIST Phase equilibria diagrams. CD-ROM database, ver. 3.2, NIST Standard Reference Database 31, The American Ceramic Society, 2008.

/7/ D.C. Kaseman, A. Retsinas, A.G. Kalampounias, G.N. Papatheodorou, S. Sen: *Q-speciation and Network Structure Evolution in Invert Calcium Silicate Glasses*. J. Phys. Chem. B, 119 (2015) 8440-8445

/8/ A. Retsinas, A.G. Kalampounias, G.N. Papatheodorou: *Glass formation and Raman spectra of CaO–SiO_2 glasses towards the orthosilicate limit*. Journal of Physics and Chemistry of Solids 99 (2016) 19–24.

Photoluminescence properties of Ce^{3+}-doped and $Ce^{3+}/Mn^{2+/4+}$ co-doped $Y_3Al_5O_{12}$ phosphors obtained by crystallization of yttrium aluminate glass with eutectic composition

K. Haladejová-Mihaldová[1], R. Klement[1], M. Parchovianský[2], A. Prnová[3], J. Valúchová[3], D. Galusek[3]

[1] Department of Functional Materials, Centre for Functional and Surface Functionalized Glass, Alexander Dubček University of Trenčín, Študentská 2, SK-911 50 Trenčín
(E-mail: robert.klement@tnuni.sk)

[2] Department of Coating Processes, Centre for Functional and Surface Functionalized Glass, Alexander Dubček University of Trenčín, Študentská 2, SK-911 50 Trenčín

[3] Vitrum Laugaricio – Joint Glass Centre of IIC SAS, TnU AD and FCHPT STU, Centre for Functional and Surface Functionalized Glass, Alexander Dubček University of Trenčín, Študentská 2, SK-911 50 Trenčín

ABSTRACT

The glass in the system Y_2O_3-Al_2O_3 with eutectic composition (76.86 mol. % (60 wt. %) Al_2O_3 and 23.13 mol. % (40 wt. %) Y_2O_3) was prepared by flame-spraying synthesis in the form of glass microspheres form precursor powder synthesized by sol-gel method. The doping level was kept at 0.25 at. % of Ce^{3+}. The prepared glass microspheres with composition Y40A60Ce0.25 were found to be XRD amorphous within detection limit. The DSC analysis revealed the two exothermic effects corresponding to crystallization of the sample Y40A60Ce0.25 at characteristic temperatures; peak 1: T_{x1} = 923 °C (onset), T_{p1} = 936 °C (peak), peak 2: T_{x2} = 989 °C and T_{p2} = 1000 °C, respectively. The origin of the two crystallization peaks (exothermic effect) was examined by high temperature XRD (HT XRD) that revealed the crystallization of YAG phase ($Y_3Al_5O_{12}$) up to 1200 °C. The crystallization of α-Al2O3 phase was observed at temperatures above 1300 °C. The both exothermic effects in DSC trace thus unusually correspond to YAG phase crystallization. The crystallization kinetics of prepared glass was interpreted in terms of nucleation growth Johnson–Mehl–Avrami–Kolmogorov (JMAK) model. The polycrystalline phosphors were prepared from the glass by controlled crystallization at selected temperatures. The photoluminescence properties of glass and polycrystalline phosphors were studied in detail. The emission spectrum of Ce^{3+} doped glass Y40A60Ce0.25 under UV excitation at 345 nm exhibits intensive blue emission; broad emission band in spectral range of 365-500 nm with the emission maximum at 407 nm. As temperature of the heat-treatment increases, the intensity of blue emission decreases, indicating that the Ce^{3+} ion is embedded into YAG crystal host. The PL emission spectra (λ_{exc} = 455 nm) of samples heat-treated at different temperatures show typical broad emission band centred at ~550 nm and PL emission intensity depends strongly on the treatment temperature. The maximum of the emission intensity was achieved for polycrystalline sample treated at 1200°C/3h. The luminescence decay of the prepared glass was well fitted with double-exponential function with lifetimes of 8 ns and 34 ns, respectively. The average lifetime of blue emission was found to be 31 ns. The green-yellow luminescence decay of the crystalline samples with Ce^{3+} ions embedded into YAG crystal host, monitored at 525 nm (under 444 nm excitation), was found to be single-exponential with the lifetime of 61 ns. The temperature dependence of the luminescence intensity of polycrystalline sample was similar as for commercial phosphor, at temperature over 150°C even better thermal behaviour was observed. More than 70% of original PL intensity at RT was achieved at temperature 300°C for sample treated (crystallised) at 1200°C/3h, while commercial phosphor exhibit around 60% of the RT PL intensity at that temperature.

To increase the intensity of orange/red emission in the phosphors PL spectra, the co-doped Ce^{3+}/Mn^{2+} phosphors with different Mn^{2+} concentration in glass (form 0.5 up to 4 at. % of Mn^{2+}) were prepared and characterised. The two cases were studied: charge compensated system with the $2Al^{3+} \rightarrow Mn^{2+} + Si^{4+}$ substitution and charge non-compensated system. In case of charge compensated system, based on the spectral overlap of the excitation spectra of Ce^{3+} - doped and Mn^{2+} -doped samples, the excitation wavelength 420 and

455 nm was selected. With increasing Mn^{2+} concentration in the host matrix the orange emission due to Mn^{2+} ions in octahedral coordination environment increases as documented by broader plateau of the overall emission (Fig. 1). On the other hand, the PL intensity of the Ce^{3+} ions decreases quite significantly due to the energy transfer (ET) between Ce^{3+} and Mn^{2+} ions. Based on the lifetime data of the Ce^{3+} emission, the efficiency of the energy transfer was estimated to be around 15%. The increasing Mn^{2+} concentration also decreases the luminescence quantum yield. In case of charge non-compensated system, the strong emission in the 625-700 nm was observed, indicating the presence of Mn^{4+} ions in the host matrix. Due to the spectral overlap of the excitation spectra of the Ce^{3+} and Mn^{4+} ions in the NUV and blue spectral region, the studied samples were excited at 342 and 450 nm, respectively. When samples excited by UNV light at 342 nm, the significant increase of the emission in red spectral region was observed. On the other hand, as in the previous case, the emission intensity due to the Ce^{3+} ion rapidly decreases as a result of significant energy transfer from Ce^{3+} to Mn^{4+} ions. At blue light excitation, only small increase of the red emission was observed together with significant reduction of Ce^{3+} emission. Due to the ET between the sensitizer (Ce^{3+}) and activator (Mn^{2+}/Mn^{4+}) ions it is reasonable to avoid co-doping in the studied system and instead to use the blend of the phosphors containing the separate luminescence ions in the same host matrix.

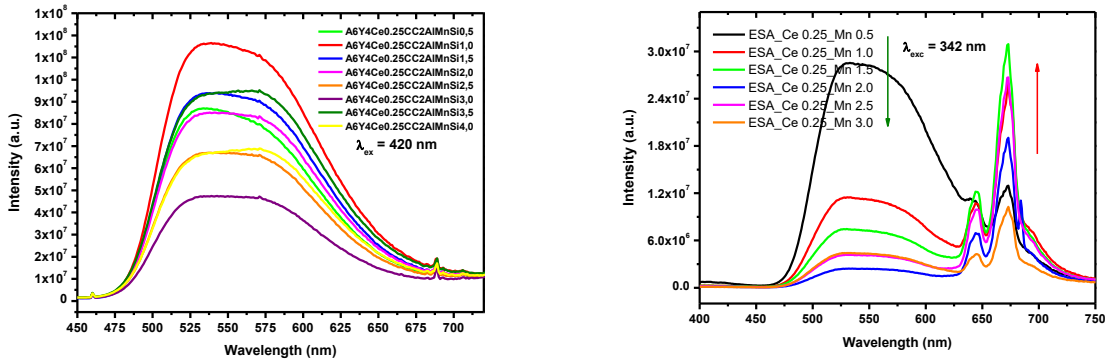

Fig.1: The PL emission spectra of charge-compensated (left) and non-compensated system (right)

Keywords: aluminate glass, YAG, Ce^{3+}-Mn^{2+} doped glass, photoluminescence, lifetime, phosphors, pc-WLED, white light.

Acknowledgment: The financial support of the work by the project VEGA 1/0527/18 is gratefully acknowledged. This work was supported by the Slovak Research and Development Agency under the contract no. APVV-17-0049.

This paper is a part of dissemination activities of project FunGlass.
This project has received funding from the European Union´s Horizon 2020 research and innovation programme under grant agreement No 739566.

HP sintering of yttrium-aluminate glass microspheres

Anna Prnová[1], Jana Valúchová[1], Milan Parchoviansky[2], Peter Švančárek[1], Robert Klement[2], Dušan Galusek[2]

[1]Dpt. VILA – Join Glass Centre of the IIC SAS, TnUAD, FChPT STU, Študentská 2, 911 50 Trenčín, Slovakia
[2]FunGlass, A. Dubček University of Trenčín, Študentská 2, 911 50 Trenčín, Slovakia

anna.prnova@tnuni.sk

ABSTRACT

Rare earth aluminate-based materials with eutectic microstructures represent an interesting approach to ceramics with important mechanical properties (hardness, fracture strength /toughness), thermal stability and creep resistance at elevated temperatures. These properties are attributed to strong eutectic interfaces between present phases and designate these materials for various aerospace (jet aircraft engines) and industrial (high efficiency power generation gas turbines components) applications. The combination of precipitation method and flame synthesis was used for preparation of glass microspheres with eutectic composition in system Al_2O_3-Y_2O_3 in our previous work [1]. The prepared microspheres were HP (hot press) sintered at different temperatures and different holding times. IR transparent ceramics and glass ceramics with fine two phase microstructure with Al_2O_3 and YAG phases percolating at submicrometre level and with hardness exceeding 15 GPa resulted from the experiments. In this work, the yttrium-aluminate glass microspheres with eutectic compositions were prepared by combination of sol-gel Pechini [2] method and flame synthesis to achieve a better compositional homogeneity of glass microspheres and improved mechanical properties of final bulk ceramic materials. The prepared glass microspheres were hot-press sintered at different conditions. The hardness and fracture toughness of prepared ceramics materials was measured and final microstructures were studied by SEM analysis (Fig.1). From comparison of results is clear, that higher pressure and holding time 30 min increasing of mechanical properties in samples sintered at temperatures ≥1300 °C. The highest values of hardness 18.0 ± 0.7 GPa and of fracture toughness 4.9 ± 0.3 MPa.m$^{1/2}$ was obtained in sample sintered at 1600 °C, pressure 80 MPa and with holding time 30 min. Similarly, higher values of hardness 16.3 ± 0.8 GPa, fracture toughness 5.5 ± 0.8 MPa.m$^{1/2}$ were obtain in sample sintered at 1600 °C, pressure 30 MPa for 30 min. Also in both cases the coarsening of the microstructure was observed by SEM analysis and presence YAG and α-Al_2O_3 crystalline phases in samples was confirmed by XRD analysis. These results indicates, that sintering of samples at higher temperatures and for longer time causes the growth of α-Al_2O_3 grains and formation of YAG/Al_2O_3 microstructure, where YAG grains are reinforced by well-connected α-Al_2O_3 matrix.

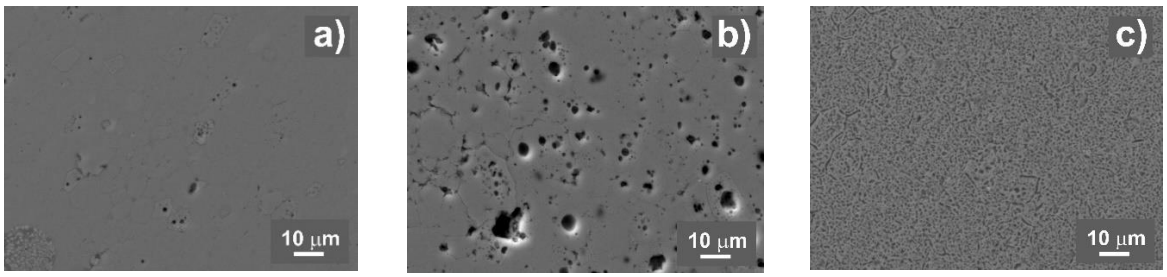

Fig.1 SEM micrographs of samples sintered at 1050°C, 80 MPa for 30 min (a), at 1600°C, 30MPa for 30 min (b) and at 1600°C, 80 MPa for 30 min (c)

Possibility of preparation of ceramic materials with fine-grained (submicron) microstructure and interesting mechanical properties by hot-press sintering of glass microspheres was confirmed.

Keywords: SEM, Vickers hardness, yttrium-aluminate glasses

Acknowledgment:

This paper is a part of dissemination activities of project FunGlass.
This project has received funding from the European Union´s Horizon 2020 research and innovation programme under grant agreement No 739566.
The financial support of this work by the projects APVV 0014-15, VEGA 1/0527/18, VEGA 2/0026/17 is gratefully acknowledged.

References:

[1] A. Prnová, D. Galusek, M. Hnatko, J. Kozánková, I. Vávra, Composites with eutectic microstructure by hot pressing of Al_2O_3-Y_2O_3 glass microspheres, Ceramics – Silikáty, 55 (2011) 208-213
[2] M.P: Pechini, Method of preparing lead and alkaline-earth titanates and niobates and coating method using the same to form a capacitor, U. S. Pat. No. 3 330 697, July 11 (1967)

Sintering experiments and luminescent properties of Zn2+ doped Y2O3

Peter Švančárek, Robert Klement, Monika Michálková and Dušan Galusek

FunGlass - Centre for Functional and Surface Functionalized Glass, Alexander Dubček University of Trenčín, Študentská 2, 911 50 Trenčín, Slovak Republic

(E-mail: peter.svancarek@tnuni.sk)

ABSTRACT

Y2O3 ceramics have been studied for many years because of their promising properties like high corrosion resistance, high melting point (2425°C), low thermal expansion coefficient and relatively high heat conductivity which can be critical for temperature management. Having cubic crystallographic unit, it is easier to create transparent ceramics since it is isotropic environment for electromagnetic radiation. Applications ranges from transparent windows to missile domes, bulb envelopes, and laser hosts[1,2]. When compared to other transparent materials such as Al_2O_3, AlON and $MgAl_2O_4$ (spinel), the Y_2O_3 has a far lower emissivity and a smaller absorption coefficient in the IR part of spectra at elevated temperatures[3]. These characteristics make it an excellent IR window material for high-temperature applications.

The starting fine grained Y_2O_3 powder was produced by PENGDA with reported particle size of 150nm. Isopropanol based suspension was prepared with 5 vol% of yttria, stabilized by PEG (1wt% of yttria mass). Suspension was dispersed by ultrasonication for 8 minutes with cycle 5(discontinuous ultrasonication). Particle Size Analyzer (90Plus, f. Brookhaven) was used to determine the level of disperzation. Analysis showed that we had reached 558nm +- 55nm particle size which is far from mean grain size of 150nm declared by Pengda manufacturer and even further from grain size of about 80nm determined by SEM. Suspension was pressure filtrated at about 50 MPa pressure to obtain green body pellets. Then the pellets were dried in oven at 40°C for 12 hours.

Green body pellets underwent the sintering experiments in Netzsch TMA 402F1 in ambient atmosphere and vacuum with following regimes:

1. In air: 10°C/min to 1100°C; followed by 5°C/min to 1550°C and 1hour of dwell time. The free cooling in furnace followed. Graph 1a.
2. In vacuum: 10°C/min to 1350°C and 2hours of dwell time followed by free cooling. Graph 1b.

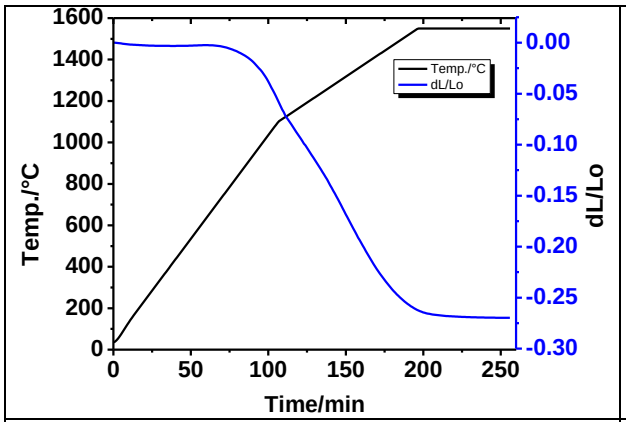

Graph 1a. Sintering experiment in air

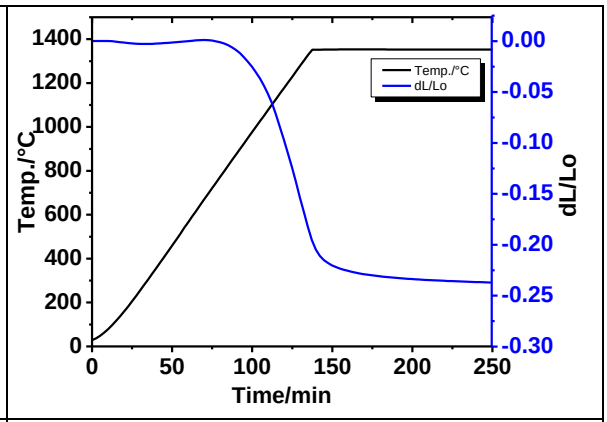

Graph 1b. Sintering experiment in vacuum

After sintering, the homogeneity of sintered specimens was evaluated visually with help of crossing light. The density (measured in water) reached 98.4% at sintering in air and 98% at sintering in vacuum. This difference was probably observed because of the settable temperature at vacuum sintering was 200°C less than the settable temperature at air sintering.

SEM images (Fig.1a and 1b) have shown fine microstructure without pores. Paradoxically, the median particle size was observed to be smaller for specimen sintered in air at 1550°C. It could be explained by length of dwell time after reaching the end density during sintering which was two times longer for vacuum sintered specimen compared to air sintered specimen.

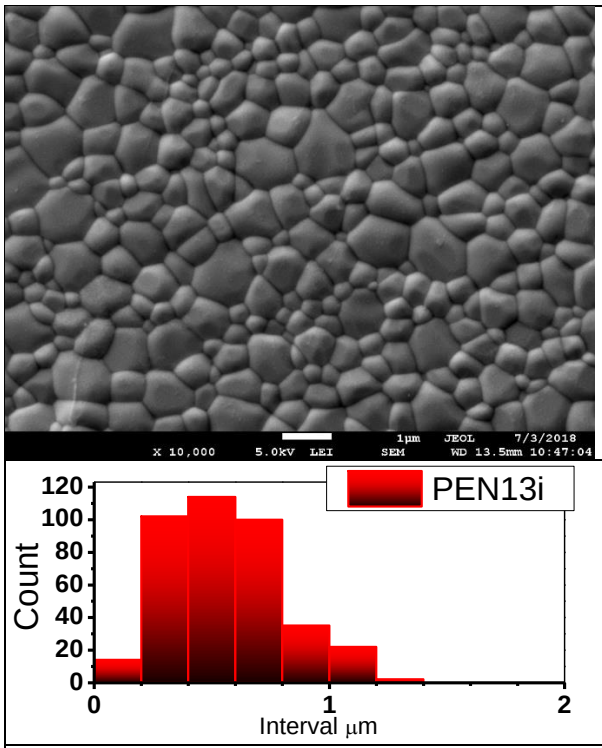

Fig.1a. SEM of in air sintered specimen

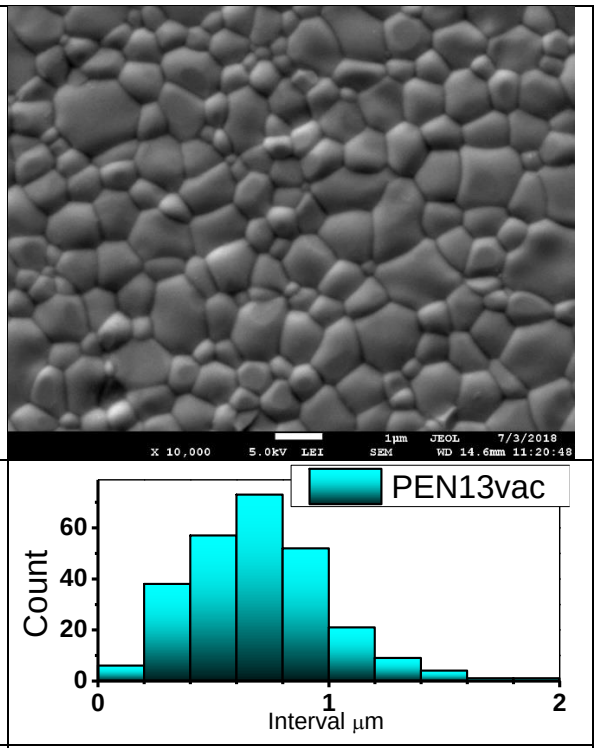

Fig.1b. SEM of in vacuum sintered specimen

First experiments with Zn^{2+} dopation were made by infiltration of presintered Y_2O_3 pellets. Presintering was made in ambient atmosphere using following regime: heating by the rate of 10°C/min to 1000°C, dwell time 1 hour which was followed by free cooling. The density was measured based on dimensions of pellets and their mass. Concentrations of doping zinc acetate solutions were adjusted according to the porosity of presintered pellets. The level of dopation was adjusted to 0.25, 0.5, 1 and 2 at. % of Zn^{2+}. After 5 hours of infiltration, the pellets were dried and sintered using following regime: heating by the rate of 10°C/min to 1400°C, dwell time 2 hours which was followed by free cooling.

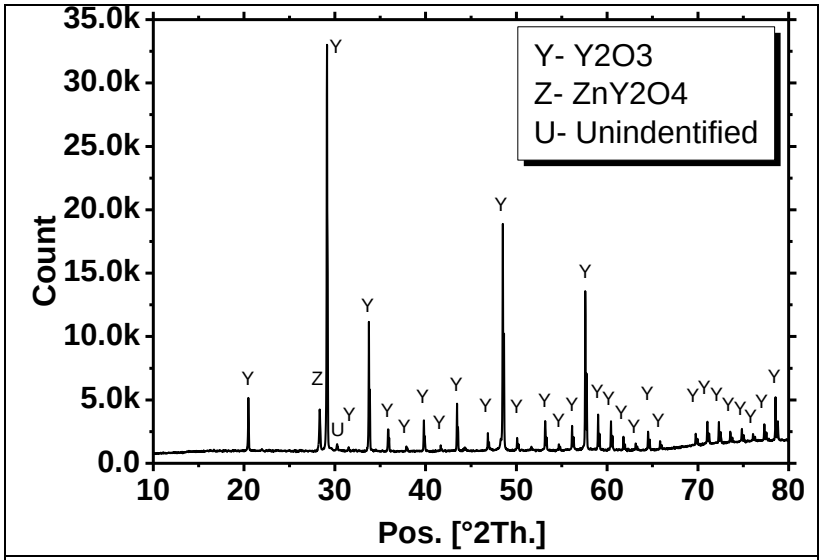

Graph 2. XRD analysis

The XRD analysis was made to determine whether new phases had emerged during sintering Y_2O_3 with addition of ZnO (Graph 2). The main phase was identified as Y_2O_3. There was also observed one relatively strong peak which might belong to orthorhombic ZnY_2O_4 phase[4].

Preliminary fluorescence spectra measurements showed the broad band emission centered at around 555 nm (warm white light emission) when the samples were excited by 378nm UV radiation.

The future work plans involve the optimization of pellet infiltration by optically active metal cations, the optimization of sintering process and application of HIP to reach fully transparent specimens.

Keywords: Pressure filtration, Thermomechanical analysis, Y2O3 ceramics

Acknowledgment:

This paper is a part of dissemination activities of project FunGlass.
This project has received funding from the European Union´s Horizon 2020 research and innovation programme under grant agreement No 739566, SAS-MOST JRP 2015/6, VEGA 2/0026/17 and VEGA 1/0527/18.

References:

[1] An, A. Ito, T. Goto, Transparent yttria produced by spark plasma sintering at moderate temperature and pressure profiles, J. Eur. Ceram. Soc. 32 (2012) 1035–1040
[2] H. Zhang, B.N. Kim, K. Morita, H. Yoshida, K. Hiraga, Y. Sakka, Fabrication of transparent yttria by high-pressure spark plasma sintering, J. Am. Ceram. Soc. 94 (2011) 3206–3210
[3] M.E. Thomas, R.I. Joseph, W.J. Tropf, Infrared transmission properties of sapphire, spinel, yttria, and ALON as a function of temperature and frequency, Appl. Opt. 27 (1988) 239–245
[4] Bidhu Bhusan Das, Venugopal Potu & Govinda Rao Ruppa, Synthesis, crystal structure and magnetic studies of ZnY_2O_4 oxide, Indian Journal of Pure & Applied Physics Vol. 53, June 2015, pp. 399-403

Functionalization of glass by sol-gel layers

Plško A.[1], Pagáčová J.[2], Papučová I.[2], Čierniková M.[1], Kuklová A.[1]

[1*] FunGlass – Centre for Functional and Surface Functionalized Glass, Alexander Dubček University of Trenčín, Študentská 2, 911 50 Trenčín, Slovakia
(*E-mail: alfonz.plsko@tnuni.sk)
[2] Faculty of Industrial Technologies in Púchov, Alexander Dubček University of Trenčín

ABSTRACT

The demands for flat glass are still at high-level, because this glass is exposed to the effect of surrounding environment. Fulfilment of these demands is commonly carried out by „funcionalization“. Functionalization is used for preparation of anti-reflective and reflective glass and in some cases, colour as well as self-cleaning glass can be involved there.

The present study deals with determination of the sol composition effect on antireflection and hydrophobicity of inorganic-organic films in “tetraethoxysilane (TEOS) - triethoxy(octyl)silane (OTES) - distilled water - nitric acid - isopropyl alcohol” system. The fifteen sols were prepared where the molar ratio (*K*) of the (OTES)/((OTES)+(TEOS)) varied from 0 to 0.5 and molar ratio (*R*) of the (H_2O)/((OTES)+(TEOS)) varied from 2 to 6.

For determination of “sol composition - film properties” relation, the corrected Akaike information criterion was used for model selection approach.

On the basis of selected models, the dependences of refractive index and hydrophobicity on sol composition were determined. Determined dependences were discussed from the aspect of possible deposition application on flat glass.

Keywords: Sol-gel, Films, Glass, Functionalization

Acknowledgment:

This paper is a part of dissemination activities of project FunGlass.
This project has received funding from the European Union´s Horizon 2020 research and innovation programme under grant agreement No 739566.

Yttria nanopowders for transparent yttria ceramics prepared by precipitation sol-gel method

Nibu Putenpurayil Govindan[1], **Monika Michálková[2]**, **Dušan Galusek[1]**,

[1]Centre for functional and surface functionalized glass
Alexander Dubcek University of Trencin, Slovak Republic
[2]Institute of inorganic chemistry, Slovak academy of science
Bratislava, Slovak Republic

Ce^{3+}-doped Y_2O_3 nanopowder was synthesized via precipitation method [1-2], using different molar concentrations of ammonium aqueous solution (0.5M, 1M, 1.5M) as precipitation agent. The aqueous nitrate solution of Y^{3+} was prepared by dissolving yttria powders (99.99 %) in diluted nitric acid (HNO_3) and deionized water under stirring and heating, then diluted into 0.1 M with deionized water. The solution of Ce^{3+} was prepared by dissolving cerium nitrate (99.99 %) in deionized water and then diluted into 0.1M with deionized water. The mixed metal nitrate solution was dripped into ammonium solution, under continuous rapid stirring, ensuring there was sufficiently high excess of ammonia to eliminate any pH fluctuations throughout the process. The mixed solution turned to opaque white slurry. After 12 h aging the slurry was vacuum filtered through filtration paper and the resulting white precipitate was washed with distilled water, dried overnight in air at 100 °C, crushed and ground in an agate mortar and pestle, and calcined in air for 3 h at 700 °C (heating rate 10°C/min). Partly agglomerated powders with the primary size of Y_2O_3 nanoparticles 55 nm and with cubic crystal structure were prepared. The optimum concentration of ammonia (precipitation agent) was found to be 0.5 M.

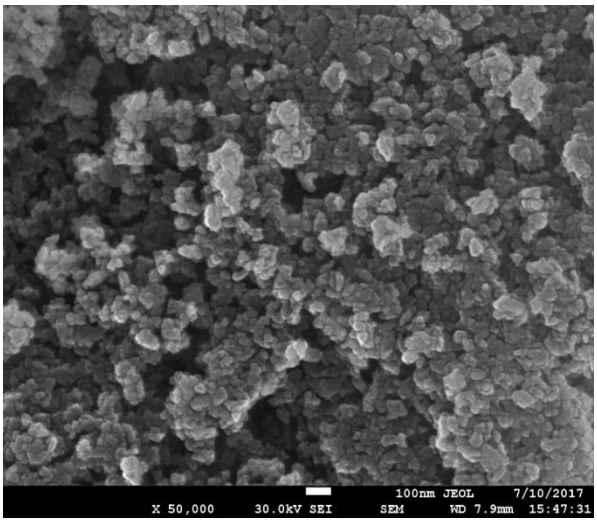

Fig 1. SEM micrograph of the prepared Y_2O_3 powder

Ultrasonication (20 kHz) was then used to de-agglomerate prepared nanopowder in ammonium solution with pH value 11. Three different dispersants Dolapix CE 64, Darvan CN, and Polyethleneglycol (PEG) were tested, respectively. The particle size distribution and Zeta potential were determined as a function of sonication time and pH.

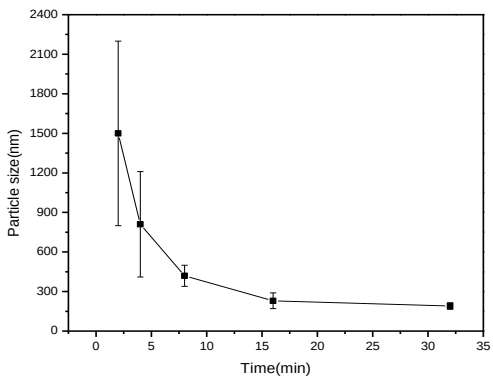

Fig 2. The change of particle size distribution of the Y_2O_3 powder with the sonication time

Figure 2.summarizes the changes in particle size distribution of yttria powder with the sonication time. Extension of the ultrasonication time results in significant reduction of both the mean size of powder particles, and the width of the particle size distribution, indicating de-agglomeration of the yttria powder. The error bar on graph represents the particle size distribution at different time interval. The best results were achieved after 32 minutes' sonication time. However, the mean size of 200 nm clearly shows that the powder was not de-agglomerated down to primary particle size (50 nm), and hard agglomerates with the diameter of about 200 nm are still present.

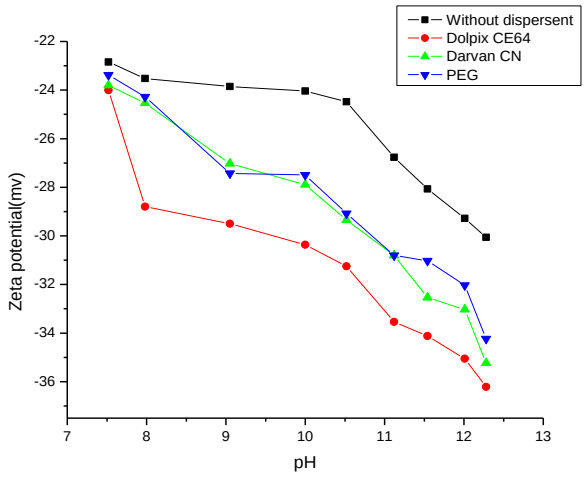

Fig.3.The results of Zeta potential of yttria suspensions with different dispersants

The zeta potential of Y_2O_3 suspension with different dispersant (2 wt. % of Dolapix CE 64, PEG or Darvan CN) as a function of pH is depicted in Fig. 3. According to literature, the stability of the particles is achieved if the absolute value of the zeta potential is higher than 30 mV [3]. The ammonia-water based Y_2O_3 suspension without dispersant shows zeta potential indicative values close to -30 mV. However, a suspension with a maximum zeta potential value of -36 mV was achieved when Dolpaix CE dispersant was added. The results of sedimentation tests confirmed better stability of the suspension with added Dolapix CE64 dispersant compared to Darvan CN and PEG stabilised suspensions. Dolapix CE64 stabilized suspensions were selected for further experiments. Green compacts prepared by vacuum-pressure filtration at the applied pressure of 20 MPa with relative density 43 % were prepared.

Keywords: Transparent ceramics, Y_2O_3, Zeta potential

ACKNOWLEDGMENT

This paper is a part of dissemination activities of FunGlass European Union´s Horizon 2020 research and innovation programme under grant agreement No 739566. The financial support of this work by the grants VEGA 2/0026/17, and SAS-MOST 2015-06 is gratefully acknowledged.

REFERENCES

[1] D. Sordelet, *Journal of Colloid and Interface Science*, 122, 47-59, **(1988)**.
[2] M. Ciftcioglu, *J. Am. Ceram. Soc*, 70 ,329-334 **(1987)**
[3] D.C.Grahame, *Chemical Review*, 41,441-451 **(1987)**

EFFECTS OF TEST PARAMETERS ON THE PRODUCTION OF HEXAGONAL BORON NITRIDE BY DCRN METHOD

Fulden Doğrul[1], A. Şükran Demirkıran[2] and Ali Osman Kurt[2]

[1] Department of Biomaterials, Centre for Functional and Surface-Functionalized Glasses, Alexander Dubcek University in Trencin (E-mail: fulden.dogrul@tnuni.sk)

[2] Sakarya University, Engineering Faculty, Department of Metallurgy and Materials Engineering 54187, Sakarya / Turkey

ABSTRACT

Hexagonal boron nitride (h-BN) is a versatile ceramic material due to its many unique physical and chemical properties, for instance low density, elevated temperature stability, high thermal conductivity, low dielectric constant, chemical inertness and lubricating property. Because of these properties, h-BN finds large application areas in industry. Carbothermal reduction and nitridation (CRN) ranked among the production methods of h-BN is an effective and economic technique. In this study, a novel method of ceramic powder production, so called dynamic carbothermal reduction-nitridation (DCRN) was performed and effects of the different test parameters were examined in producing h-BN. The granules were prepared from the mixture of boron oxide (B_2O_3), carbon and calcium carbonate ($CaCO_3$). These granules were placed in a graphite reactor, where they reacted with nitrogen gas in the atmosphere controlled tube furnace, which alumina tube was rotating with controlled speed. The effects of test conditions such as temperature, exposure time and rotation speed of the reactor on the formation of boron nitride were examined. The reaction products were characterized by X-ray diffraction (XRD) and Field Emission Scanning Electron Microscopy (FESEM). The optimum production conditions according to XRD analyses and FESEM examinations were determined as 1400 °C for 2 h reaction with rotational rate of 4 rpm.

The XRD patterns of reaction products obtained at different temperatures for 2 hours are shown in Figure 1(a). The intensity and width of the strongest h-BN diffraction line at 2θ = 26.627° increased with increasing reaction temperature. Both crystallite size and lattice strain increase the peak width and intensity and shift the 2θ peak position accordingly [Zak et al., 2011]. Therefore, the peak broadening was attributed to decreasing size of BN crystallites. The products synthesised at 1400 °C contained h-BN, C and some glassy phase.

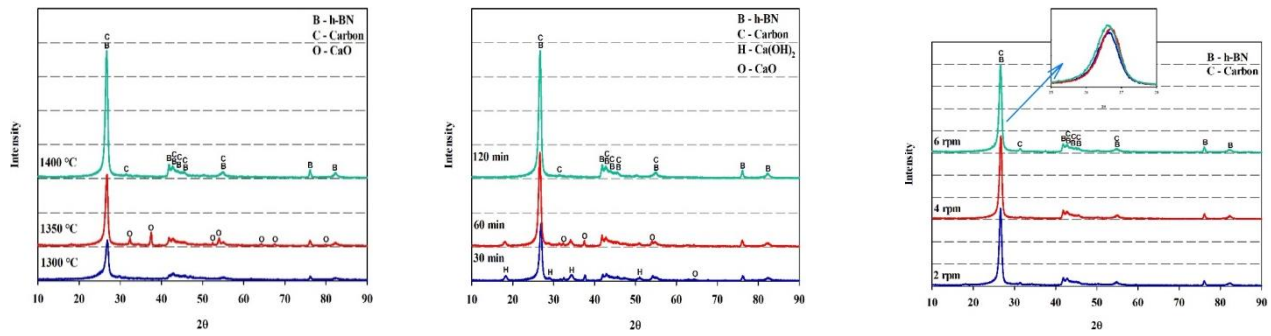

(a) (b) (c)

Figure 1: (a) The XRD patterns of reaction products obtained at different temperatures, (b) The XRD patterns of reaction products at various reaction times at 1400°C. (c) XRD patterns obtained at different rotating rates for 2 hours at 1400°C

The XRD patterns for different reaction time are shown in Figure 1 (b). The reaction products obtained at 1400 °C after 30 and 60 minutes contain C, h-BN, Ca and $Ca(OH)_2$ phases. Formation of the $Ca(OH)_2$ phase is atributed to hydratation of free lime after the synthesis. The intensity and width of the main h-BN diffraction line increased with increased duration of the reaction.
The phases formed at all rotational speeds are h-BN, C and glassy phase and the intensity and width of the main h-BN diffraction maximum increase with increasing reactor rotation speed. However, agglomeration was observed in the powders rotated at 6 rpm.

To get rid of the glassy and undesirable other phases found in the reaction products, samples were subjected to chemical activation using 5 M HCl acid solution for 15 hours. After the chemical activation the samples were washed, filtrated and dried before exposure to oxidation at 800 °C for 15 h to remove the unreacted C. The XRD pattern which belongs to reaction products produced with DCRN method and the XRD pattern of reaction products obtained after carbon combustion are shown in Figure 2.1. As seen in the Figure 2.1(a), the reaction products prepared by the DCRN method contain both BN and C phases. After carbon combustion, all the peaks were indexed as hexagonal BN. The peak width and intensity changes at the XRD pattern of products obtained after carbon combustion. The prominent (002) plane indicate the existence of well-stacked layered structures in the h-BN powders [Yang et al., 2005].

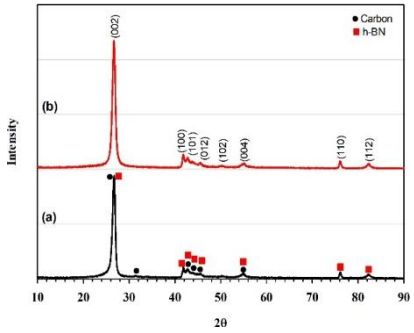

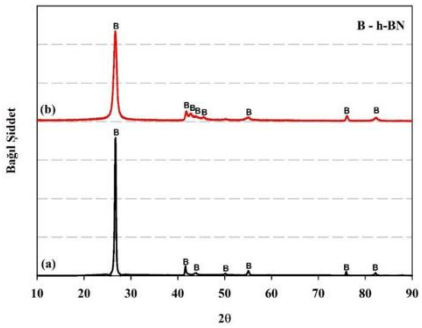

Figure 2.1: XRD patterns of (a) the reaction products produced with DCRN method and (b) products obtained after carbon combustion, Figure 2.2: XRD patterns of (a) commercial product of h-BN, final product obtained by DCRN

The FESEM micrographs of reaction products and final powder products are shown in Figure 3. After chemical activation and oxidation process, the flake morphology of h-BN particles is clearly visible in the micrograph. The flakes are restricted to nanoscale in thickness.

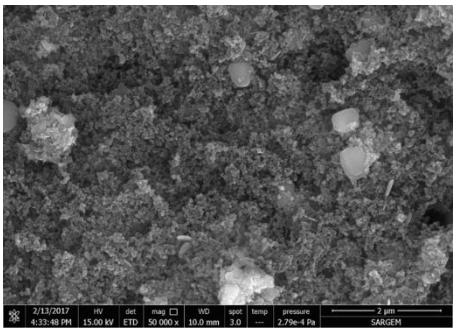

(a)

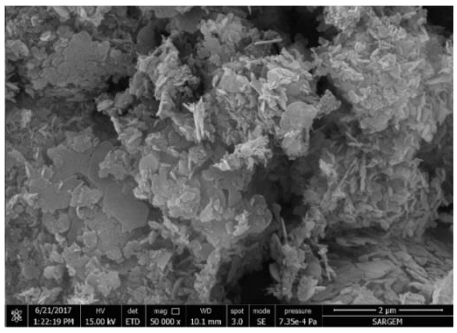

(b)

Figure 3: The FESEM micrograph of (a) reaction product obtained by DCRN , (b) final powder products. (Scale bar shows 2 µm.)

Keywords: DCRN, CRN, advanced ceramics, h-BN

Acknowledgment:

This paper is a part of dissemination activities of project FunGlass.
This project has received funding from the European Union´s Horizon 2020 research and innovation programme under grant agreement No 739566.

References:

Ay, G.M., Göncü, Y., Ay, N., 2016. Environmentally friendly material: Hexagonal boron nitride, Journal of BORON, 1 (2), 66.

Chen, L., Gu, Y., Shi, L., Yang, Z., Ma, J., Qian, Y., 2004. A room-temperature approach to boron nitride hollow spheres, Solid State Communications, 130, 537.

Zak, AK., Majid, W.H.A., Abrishami, M.E., Yousefi, R., 2011. X-ray analysis of ZnO nanoparticles by Williamson-Hall and size-strain plot methods, Solid State Sciences, 13 (1), 251

Yang, Z., Shi, L., Chen, L., Gu, Y., Cai, P., Zhao, A., Qian, Y., 2005. Synthesis, characterization and properties of novel BN nanocages from a single-source precursor, Chemical Physics Letters, 405, 229.

An overview: Polymer Derived Ceramic (PDC) Coating on stainless steel

Nitin Kamble, Dušan Galusek
FunGlass – Centre for Functional and Surface Functionalized Glass, Alexander Dubček University of Trenčín, Študentská 2, 911 50 Trenčín, Slovakia
(E-mail: nitin.kamble@tnuni.sk)

Abstract

Metallic component especially stainless steel exposed highly reactive and corrosive environments such as high temperature oxidation, acidic corrosion, degrade or fail quickly leading to enormous economical loss. Common solution to this problem is either using expensive alloys or replacing corroded parts frequently. Alternatively, applying corrosion resistance coating offers promising way to protect metallic substrate from corrosion and extended their service life. Conventional methods of making coatings include, but not limited to, thermal spraying, welding, electroplating, chemical vapor deposition (CVD) [1] and physical vapor deposition (PVD) [2], all of which are high energy consumption techniques. Recently polymer derived ceramics (PDCs) have gained greater attention due to its properties like easy application on substrates of any shape, low temperature processing and the potential to tailor the properties via microstructure and composition design. Preceramic polymers are attractive for coating applications because of their strong adhesion to polymers, metals, and ceramics, which is attributed to the formation of covalent bonds between precursors and coated surfaces. Further, these compounds, in polymeric and ceramic states, possess outstanding protective properties that are necessary for environmental barrier applications [3-6]. A critical thickness exists for polymer derived ceramic coatings. Below this thickness value, the coatings remain intact, dense and adherent. If the thickness exceeds this value, cracking and delamination of the coatings occur during pyrolysis. Different preceramic system with pyrolysis temperature is tabulated in table-1

Table 1
Well-known PDC coating systems.

Precursor systems	Substrate	Temperature	Environment	Reference (Published year)
Polyhydridomethylsiloxane (PHMS)	Carbon Steel/Stainless Steel	600 °C/700 °C	Air	[5] (2009)
Polysilazane	13CrMo4-5 (AISI A182) & X5CrNi18-10 (AISI 304)	700 °C	Air	[6] (2012)
PHPS polysilazane/ ABSE polycarbosilazane	Stainless steel (AISI 304)	1000 °C	Air	[7] (2009)
Polyhydridomethylsiloxane (PHMS)	Stainless steel (AISI 304)	800 °C	Air	[8] (2012)
Polyhydridomethylsiloxane (PHMS)	316 stainless steel	800 °C	Air	[9] (2008)
Polymethoxymethylsiloxane/ Hydroxy-terminated linear dimethylpolysiloxane	Stainless Steel (#1.4301 DIN EN 10027-2)	1000 °C	Argon	[10] (2010)
Polyhydromethylsiloxane PHMS	Stainless Steel 316 (UNS S31600)	800 °C	Air	[11] (2014)

The greatest disadvantage of polymer derived ceramics is the shrinkage of the polymer during pyrolysis, which can be higher than 50% by volume. Residual stresses caused by the high volume shrinkage lead to the formation of defects, cracks or even delamination of the coatings. By adding passive fillers like SiC, BN, ZrO_2, Al_2O_3[7-8] and/or active fillers like Nb, Ti, $TiSi_2$, Hf [9] the volume change from polymer to ceramic conversion can be significantly reduced. By selecting proper filler particle with thermal expansion coefficient which matches with thermal coefficients of substrate, overcome the limitation of residual stresses. With help of fillers it is possible to generate coatings with additional functionalities like special friction properties, electrical or thermal conductivity or catalytic activity. Table-2 Different fillers and glass wth their thermal expansion coefficents[10].

Material	Average particle size d_{50} (mm)	Thermal expansion coefficient α (10^{-6}/K)	Softening point (° C)	Density (g/cm^3)
BN	0.7	3.5–4	–	2.25
Si_3N_4	0.6	2.5–3.5	–	3.2
ZrO_2	1	9–13	–	5.7
Glass 8472	9.7	12	360	6.7
Glass G018-198	9.9	9–10	444	6.6
Glass 8470	3.3	10	570	2.8
Glass G018-311	3.1	10	770	3.8

For this, different polysilazane systems, ceramic fillers and glass additives were selected and investigated as coating materials. A processing route which includes pre-treatment of the steel substrates, preparation of the coating slurry, application of the composite coating and thermal treatment in air were studied from different researcher's. The investigations show that the pre-treatment as well as the application of a polysilazane systems on steel substrates are very important to achieve well adherent composite coatings. One of them was double layer coating (i.e. bond coat and top coat), increases the adhesion of the composite coatings and further acts as diffusion barrier against oxidation during the pyrolysis step of the coating system. The critical coating thickness of the coating systems can be increased up to 100 µm, if the polysilazane and filler systems, their volume fractions and the processing parameters are tailored and optimized. Cyclic oxidation tests showed that the coating system protects steel against oxidation up to 800 ºC. The results of various studies confirm that the combination of PDCs with tailored fillers and glass systems enable the processing of thick, dense and crack-free composite coating systems. Furthermore, the double coatings can be processed in air, leading to an efficient process. These coatings are suitable as protective coatings at medium temperatures, e.g. for exhaust systems, waste incineration plants, metal or glass casting and for applications in the chemical industry.

References:

1. Cao XQ, Vassen R, Stoever D. , *J Eur Ceram Soc* 2004;**24**:1–10.
2. Bach FW, Möhwald K, Laarmann A, Wenz T. *Moderne Beschichtungsver-fahren* , Weinheim: Wiley-VCH; 2005.
3. Greil P. *Adv Eng Mater* 2000;**2**(6):339–48.
4. Colombo P, Riedel R, Soraru GD, Kleebe HJ. DEStech Publications; 2009.
5. Riedel R, Mera G, Hauser R, Klonczynski A. J Ceram Soc Jpn 2006;114(6):425–44.
6. Colombo P, Mera G, Riedel R, Soraru GD. J Am Ceram Soc 2010;97(7):1805–37.
7. Greil P. J Am Ceram Soc 1995;78(4):835–48.
8. Kraus T, Günthner M, Krenkel W, Motz G, Adv Appl Ceram 2009;108(8):476–82.
9. Scheffler M, Dernovsek O, Schwarze D, Bressiani AHA, Bressiani JC, Acchar W, J Mater Sci 2003;38(24):4925–31.
10. M.Günthner, A.d Schütz, U. Glatzel, K. Wang, R. K. Bordia, O. Greißl, W. Krenkel, G. Motz,Journal of the European Ceramic Society 31 (2011) 3003–3010.

Acknowledgment: This paper is a part of dissemination activities of project FunGlass. This project has received funding from the grant APVV 0014-15 and European Union´s Horizon 2020 research and innovation programme under grant agreement No 739566.

Preparation, investigation and characterization of polysilazane-derived (oxy)nitride coatings on steel substrate

M. Parchovianský[1], I. Petríková[1], P. Švančárek[1], G. Motz[2], D. Galusek[1]

[1]FunGlass - Centre for Functional and Surface Functionalized Glass, Department of Coating Processes, Študentská 2, 911 50 Trenčín, Slovakia
(E-mail:milan.parchoviansky@tnuni.sk)
[2]University of Bayreuth, Ceramic Materials Engineering, D-95440 Bayreuth, Germany

ABSTRACT

In this work the effect of different treatment such as sandblasting, etching on the surface or combination of these method and preparation of the coatings by dip coating and spray coating method with different volume fraction of commercial or manufactured materials is under investigation. The main goal of the treatment of steel is choose the best type of cleaning stainless steel and avoid the spallation of the base coat from the steel substrate. Stainless steel (AISI 441) was used as basic substrate. Before pre-treatment and coating process, the steel plates were cut into required dimension 1.5 cm × 1.5 cm, cleaned by six different ways. The experimental conditions of the pre-treatment of stainless steel are shown in the Tab. 1. The surface morphology and roughness parameters were observed by Raman spectroscopy with the use of the Renishaw InVia using atomic force microscope. After the pre-treatment of stainless steel follow the preparation of coatings.

PHPS (perhydropolysilazane) and Durazane 1800 (both Merck KGaA, Germany) were used like pre-ceramic precursors. In order to obtain dense and adherent coatings with sufficient protection, new types of glasses (Schott AG, Mainz, Germany) and ceramic fillers (YSZ – Inframat, USA, AYZ20) were used. The pre-treated substrates were dip-coated (Relamatic RDC 15, Switzerland) in the PHPS solution to obtain the bond-coat. The curing of the PHPS bond-coat was carried out in air at 450 °C for 1h with heating rate of 3K/min (N41/H, Nabertherm, Germany). The subsequently applied top coat was prepared by mixing defined volume fractions of a liquid polysilazane HTT1800, ceramic filler particles and glasses. Parameters like the filler and glass systems, the volume fraction of the components were varied to optimize the composite coating system. The pyrolysis of the coatings was performed in air at the temperature 850 °C with a holding time 1 h. The compositions are listed in the Tab. 2 and Tab. 3. After the pyrolysis the compositions were in detail analysed by SEM, XRD.

Tab. 1: Experimental conditions of pre-treatment of stainless steel

Shortcut	Pre-treatment of stainless steel
U	3-steps ultrasonic vibration cleaning in acetone, ethanol and deionized water (10 min)
P	Sandblasting with glass beads (70-110µm), ultrasonic cleaning
N	Chemical etching – NITAL (ethanol+nitric acid), 1min
K	Chemical etching – KROLLS REAGENT (distilled water, nitric acid, HF), 20sec
P+N	Sandblasting with glass beads + etching with NITAL
P+K	Sandblasting with glass beads + etching with KROLLS REAGENT

Tab. 2: The selected compositions with Schott glass G018-281 and precursor AYZ20

COMPOSITIONS	HTT1800 (vol. %	YSZ (vol. %)	G018-281 (vol. %)	AYZ20
D1	20	20	40	20
D2	25	20	35	20
D3	30	20	30	20

Tab. 3: The selected compositions with Schott glass G018-281

COMPOSITIONS	HTT1800 (vol. %	YSZ (vol. %)	G018-281 (vol. %)	YSZ:GLASS
C1a	20	50	30	5:3
C1b	25	46,88	28,12	
C1c	30	43,75	26,25	
C1d	35	40,63	24,37	
C2a	20	40	40	1:1
C2b	25	37,5	37,5	
C2c	30	35	35	
C2d	35	32,5	32,5	
C3a	20	30	50	3:5
C3b	25	28,12	46,88	
C3c	30	26,25	43,75	
C3d	35	24,37	40,63	

The surfaces and morphology of samples after treatment (Fig. 1a) shows that different etching and sandblasting on the stainless steel surface created different size of roughness and there is a relation between surface morphology and the kind of used reagents. It was found that pre-treatment of the substrate surface was very important for successful preparation of bond coat. Sandblasting and etching with different chemical etchants rendered the different substrate surface roughness. Atomic force microscope measurements revealed the surface roughness of sandblasted and etched stainless steel, ranged from 0.2-1.7 µm that related to ultrasonic cleaning and sandblasting, respectively. It was found that ultrasonic cleaning showed the best adhesion of PHPS to the steel (Fig. 1b).

In the case of top coat in all cases was found that addition of smaller amount of polymer HTT1800 (<30 vol. %) was not effective and spallation of top coat from bond coat was observed. With the high amount of polymer the adhesion of bond coat and top coat was good. The composite coating D3 (Fig. 3c) provides the most promising overall results. The top coat D3 was prepared with 30 vol. % of HTT1800, YSZ, and powder precursors (Al_2O_3-Y_2O_3-ZrO_2) as passive fillers and the glass system G018-281 as sealing agent. After a thermal treatment in air at 850 °C, the resultant coating with the thickness up to 40 µm is almost fully dense, with no cracking or delamination and it is expected to prevent the access of aggressive environment to the steel substrate at temperatures up to 1000 °C.

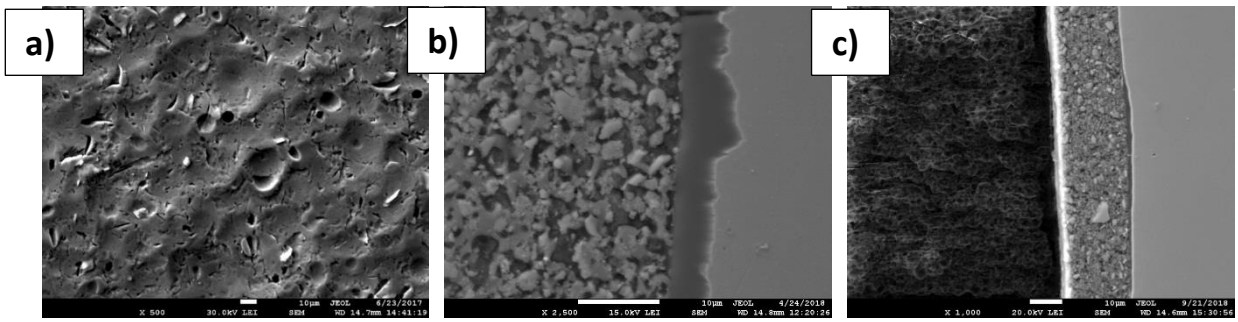

Fig. 1: Surfaces and cross-sectional SEM images a) sandblasted surface of steel, b) composition C3cU – ultrasonic cleaning, c) compositions D3U

Keywords: bond coat, PDC coatings, top coat, treatment of steel
Acknowledgment:

This paper is a part of dissemination activities of project FunGlass. This project has received funding from the the grant APVV 0014-15 and European Union´s Horizon 2020 research and innovation programme under grant agreement No 739566.

Effect of Gamma Radiation on the Chemical Durability of Glass Fibrous Insulation Used in Nuclear Power Plants

J. Vráblová[1], M. Liška[1], M. Chromčíková[1], J. Michálková[1], H. Kaňková[1], V. Soltész[2]
[1]FunGlass – Vitrum Laugaricio – Joint Glass Center of IIC SAS, TnU AD, and FChPT STU
Študentská 2, Trenčín, SK – 911 50, Slovak Republic
(E-mail: jana.vokelova@tnuni.sk, marek.liska@tnuni.sk, maria.chromcikova@tnuni.sk, jaroslava.michalkova@tnuni.sk, hana.kankova@tnuni.sk)
[2]VUEZ, Hviezdoslavova 35, P.O. Box 153, Levice, SK-943 39, Slovakia
(E-mail: soltesz@vuez.sk)

ABSTRACT

In case of an accident the emergency system of a nuclear power plant is used in order to preserve pressure of a coolant in the primary cooling circuit and to disposefrom the active zone of nuclear reactor. The system consists of the tanks filled with the boric acid solution and the pumps transporting solution to the primary cooling area. Moreover the low-pressure pumps are activated when the tanks are not able to bring the cooling solution into the system. After pumping out, the cooling solution is pumped in again from the heat exchanger placed at the bottom of the hermetic boxes. Loss of coolant accident – LOCA (damage of the primary cooling area) causes rapid increase of pressure in the hermetic boxes. Therefore the spraying system is activated. Required decrease of pressure is achieved by spraying the area of the hermetic boxes and by condensation of steam and air mixture. The glass fibers play a significant role regarding the security system of the nuclear plants. Glass fibers are mainly used as thermal and electrical insulation and in case of accident fibers get in immediate contact with cooling solution. It is well known that water solution in contact with a glass causes changes resulting in the structure transformation of glass surface, dissolution of a glass itself and formation of new glass surface layer.

The chemical durability of gamma-irradiated glass fibrous insulation commonly used in the reactor containment of nuclear power plants was tested by static leaching tests at 70, 80 and 90°C. Distilled water was used as corrosive medium. Two radiation doses, 2 and 4 MGy, were applied, the higher one roughly corresponding to 30 years of irradiation in reactor containment. The glass insulation was irradiated at low (70°C) and increased (450°C) temperatures. The results of the static leaching tests were compared with those obtained for non-irradiated native glass fibers. Therefore, the aim of the present work is the study of influence of gamma irradiation and temperature on the chemical durability of glass fibers. This will be quantified by static leaching tests of non-irradiated native glass fibers and irradiated glass fibers performed in distilled water.The detailed analysis of results of static and flow thorough leaching tests leads to the hypothesis of quasi congruent glass dissolution. Using this assumption the leaching kinetics was described by the Aagaard Helgeson equation. The kinetic parameters were obtained by the non-linear regression analysis of time evolution of leaching solution composition.

Keywords: Glass fibers, corrosion, LOCA, chemical durability, gamma radiation, static leaching tests.

Acknowledgment:

This paper is a part of dissemination activities of project FunGlass.
This project has received funding from the European Union´s Horizon 2020 research and innovation programme under grant agreement No 739566.
This work was supported by The Slovak Grant Agency for Science under grant No. VEGA 2/0088/16, VEGA 1/0064/18 and APVV 0487-11.

References:

/1/ MIŠÍKOVÁ, L. - GALUSKOVÁ, D.: *Corrosion of e-glass fibers – security factor of nuclear power plants,* Ceramics – Silikáty, *50* (2), 73-77, 2006.

/2/ CHROMČÍKOVÁ, M. – VOKELOVÁ, J. - MICHÁLKOVÁ, J. - LIŠKA, M. - MACHÁČEK, J. - GEDEON, O. - SOLTÉSZ, V.: *Chemical durability of gamma-irradiated glass fibrous insulation.* J. Nuclear Technology 193, 297-305, 2016.

/3/ SOLTÉSZ, V. - Et Al.: *Chemical durability of glass thermal insulation fibers in borate and phosphate water solutions.* Advanced Materials Research 363, 2008.

Structure and properties of glass fibers insulation used in nuclear power plants

J. Michálková*[1], J. Vokelová[1], H. Kaňková[1] M. Chromčíková[2,3], M. Liška[2,3]

[1] Central Laboratories, FunGlass, Alexander Dubček University of Trenčín, Študentská 2, SK-911 50 Trenčín, Slovakia
(E-mail: jaroslava.michalkova@tnuni.sk, jana.vokelova@tnuni.sk, hana.kankova@tnuni.sk)
[2] VILA – Joined Glass Centre of the IIC SAS, TnUAD, FChPT STU, Študentská 2, SK-911 50 Trenčín, Slovakia
(E-mail: maria.chromcikova@tnuni.sk,marek.liska@tnuni.sk)
[3] VILA, FunGlass, A. Dubcek University of Trenčín, Študentská 2, SK-911 50 Trenčín, Slovakia
(E-mail: maria.chromcikova@tnuni.sk,marek.liska@tnuni.sk)

ABSTRACT

The basic physical properties and chemical durability of glass used for production of the NUKON glass fibrous insulation were measured. This type of glass insulation is used in nuclear power plants and its properties are important for safety reasons – namely in the case of Loss Of Coolant Accidents (LOCA). During this postulated accident, the insulation can be damaged by the jet impact and carried to the screens of the emergency systems needed to cool the reactor. In this case, the fibers can be strongly corroded by particular coolant solutions and their behavior under this environment can modify the head loss of the screens. In addition corrosion products formed during contact of insulation fibers with aggressive cooling solution can cause changes, resulting in insufficient even functionless operation of the cooling system. Therefore the chemical durability of NUKON glass fibers was tested in present work by leaching corrosion tests. The coolant solution $H_3BO_3/Na_2B_4O_7$ was used as corrosive medium. The glass dissolution was followed by atomic emission spectrometry with inductively coupled plasma (ICP - OES). The low temperature viscosity was measured by the thermomechanical analysis. The temperature dependence of viscosity was described by the Andrade viscosity equation. The glass transition temperature and the thermal expansion coefficients of glass and metastable melt were determined by the thermodilatometry. The liquidus temperature was measured in the gradient furnace by the method of the first crystal. The glass density at laboratory temperature was measured by Archimedes method. The heat capacity and glass transition characteristic were determined by DSC method.

Keywords: Glass fibres, thermal insulation, LOCA, coolant solution, physical properties, corrosion.

Acknowledgment:

This paper is a part of dissemination activities of project FunGlass.
This project has received funding from the European Union´s Horizon 2020 research and innovation programme under grant agreement No 739566.
This work was supported by The Slovak Grant Agency for Science under grant No. VEGA 2/0088/16, VEGA 1/0064/18 and APVV 0487-11.

References:

/1/. A.E. LANE et al.: WCAP-16530-NP, Evaluation of Post-Accident Chemical Effects in Containment Sump Fluids to Support GSI-191, Revision 0, Westinghouse Electric Company LLC, Pittsburgh: p. 182, (2006).

/2/. OBDRLÍKOVá, V.: Koroze izolačnách vláken pro jaderné elektrárny, Diplomová práce, VŠCHT Praha, (2013).

/3/. CHROMČÍKOVÁ, M. – VOKELOVÁ, J. - MICHÁLKOVÁ, J. - LIŠKA, M. - MACHÁČEK, J. GEDEON, O. - SOLTÉSZ, V.: *Chemical durability of gamma-irradiated glass fibrous insulation.* J. Nuclear Technology 193, 297-305 (2016).

Raman spectroscopy and PCA, MCR study of heavy weathered glass

B. Hruška*[1], A. Černá [1], M. Chromčíková[2,3], V. Vargová[4] and M. Liška[2,3]

[1] Central Laboratories, FunGlass, Alexander Dubček University of Trenčín, Študentská 2, SK-911 50 Trenčín, Slovakia
(E-mail: branislav.hruska@tnuni.sk, andrea.cerna@tnuni.sk)
[2] VILA – Joined Glass Centre of the IIC SAS, TnUAD, FChPT STU, Študentská 2, SK-911 50 Trenčín, Slovakia
[3] VILA, FunGlass, A. Dubcek University of Trenčín, Študentská 2, SK-911 50 Trenčín, Slovakia
(E-mail: maria.chromcikova@tnuni.sk, marek.liska@tnuni.sk)
[4] RONA a.s.,Schreiberova 365, Lednické Rovne, SK – 020 61, Slovak Republic
(E-mail: veronika.vargova@rona.sk)

ABSTRACT

The chemical composition of a glass surface is a key factor in its interaction with the environment. Under certain exposure conditions its optical properties, chemistry and structure are modified by different weathering processes [1]. As a consequence of the interaction between the glass and a solution, irreversible changes in glass can be observed. Most important of them are as follows: dissolution of the glass, transfer of glass components into the solution, changes of glass surface composition, especially the depletion of alkali and alkali earth ions, and creation of secondary precipitated layers on the glass surface [2-3].

The corrosion products on heavy weathered surface of barium crystal glass were studied by the micro Raman spectroscopy. Spectra were recorded in the range of (200–1500) cm^{-1} by RENISHAW inVia Reflex Raman spectrometer with the Leica DM2500 microscope. The excitation 532 nm laser with 28.5 mW power was used for a spot of about 1 mm diameter.

The weathered surface was studied by lateral spectral maps recorded in the autofocus mode. The surface of approximately (0.5 x 0.5) mm was scanned into the map of the size of 12 x 12 points.

The stratified structure of glass weathered surface was studied by Raman spectra depth profiling. The series of Raman spectra were recorded with different focusing depth level ranging from surface level up to the depth of 10 μm.

After the baseline subtraction the number of independent spectral components was determined by the Principal Component Analysis (PCA). Then the spectra of pure components (so called loadings) and their relative abundances (so called scores) were determined by the multivariate curve resolution method (MCR). The corrosion products were identified by the S.T. Japan database applied to each MCR loading.

This way the following weathering/corrosion products were identified corrosion products on Table 1 were identified by the micro Raman spectroscopy on the weathered glass surface by the S. T. Japan Spectral database.

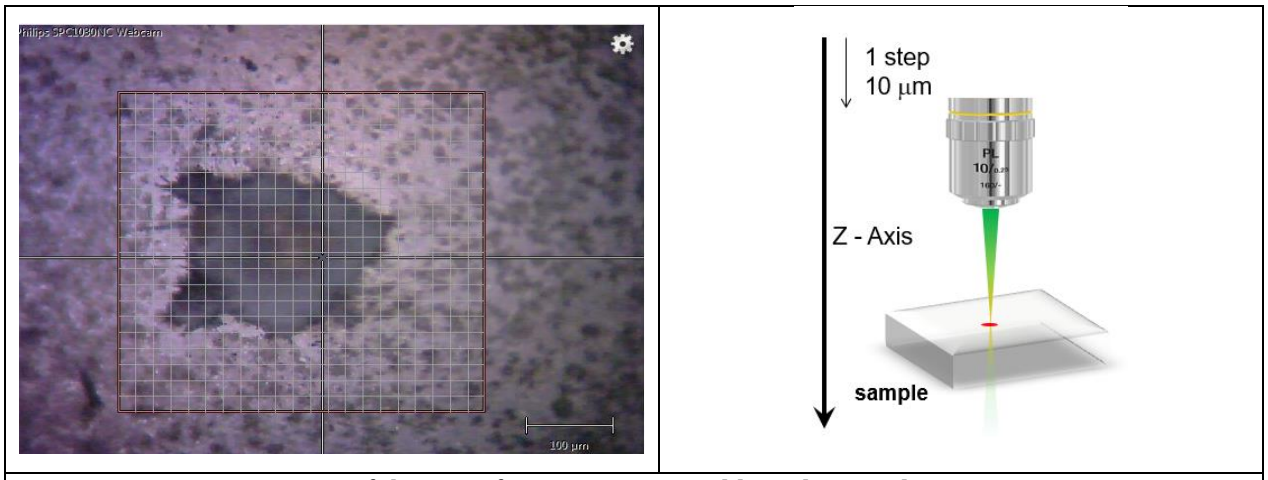

Map of the size of 12 x 12 points and lateral spectral maps

Table 1: Corrosion product

	Characterization corrosion products	
ST Japan Spectral databases	St # 931	OKENITE (hydrated calc-silicate) $Ca_5Si_9O_{23}$ x $9H_2O$
	St # 746	Pyrophyllite (aluminosilicate) $Al_2Si_4O_{10}(OH)_2$
	St # 379	Okenite (hydrated calc-silicate) $Ca_5Si_9O_{23}.9H_2O$
	St # 405	Tridymite (Silica group) SiO_2 (GSJ M35459)
	St # 187	Cordierite $Mg_2Al_3(AlSi_5O_{18})$

Keywords: Barium crystal glass, PCA, MCR, micro Raman spectroscopy, corrosion products

Acknowledgment:

This paper is a part of dissemination activities of project FunGlass.
This project has received funding from the European Union´s Horizon 2020 research and innovation programme under grant agreement No 739566.
This work was supported by The Slovak Grant Agency for Science under grant No. VEGA 2/0088/16, VEGA 1/0064/18. This work was supported by the project of Interreg program between Slovak republic and Czech republic (2014 – 2020) „*Rozvoj vzdelávacej infraštruktúry Bielokarpatskej sklárskej základne*“, ITMS code: 304011C847.

References:

/1/ N. Papadopoulos, CA. Drosou: *Influence of weather conditions on glass properties*, Journal of the University of Chemical Technology and Metallurgy 47 (2012) 429-439.

/2/ V. Petrušková, P. Vrábel, M. Liška, D. Galusková, L. Mišíková, P. Šajgalík: *Corrosion of barium and barium free crystal glass in a flow-through reactor. Glass Technology*, European Journal of Glass Science and Technology Part A 50 (2009) 258-268.

/3/ NP Mellott, CG Pantano: *A Mechanism of Corrosion Induced Roughening of Glass Surfaces*, International Journal of Applied Glass Science 4 (2013) 274-279

Novel borophosphosilicate bioactive glass composition – analysis and corrosion behavior

Petr Chrást*[1], Martin Michálek[1], Jozef Kraxner[1] and Dušan Galusek[1]

*) corresponding author: petr.chrast@tnuni.sk

1) Centre for Functional and Surface Functionalized Glass, Alexander Dubcek University of Trencin, Trencin, Slovakia

ABSTRACT

Nowadays, the tissue engineering (TE) field requires research and production of bioactive materials, which facilitate healing processes to greater extent than bioactive materials produced in earlier stages of bioactive material research (Hench's silicate Bioglass[1, 2])

The most important factors that the bioactive material has to introduce into the process of recovery or injury mitigation are creation of a chemical bond between the artificial tissue (bioactive material) and the original (maternal) tissue, and the subsequent tissue regeneration induced by the decomposition of bioactive material. Hence, the requirements for the bioactive material matrix are both to be durable to withstand the natural conditions of the human body and to be biologically degradable and non-toxic at the same time.

Glass as a bioactive material offers its dissolution in aqueous media as one of the more defined properties. It also can be fabricated into various shapes by melting or by melting and pulverizing, with subsequent pressing or 3D printing of the glass powder into the field of tissue engineering. The glass material alone does not achieve required performance in terms of tensile strength and other factors of mechanical resistance. It is therefore more preferably utilized in composite materials to increase its mechanical durability, since retaining the original mechanical properties of an implant is the key factor for its utilization *in vivo*.

Dissolution of glass matrix takes place through a sequence of reactions [3, 4]. In approximation, aqueous media react with the bridging oxygen bonds while the corrosion products (ions of glass modifiers or fragments of glass network formers) are slowly released into the surrounding environment. This changes the pH of corrosion environment, and alters the reaction kinetics. The glass surface accumulates the corrosion products either in form of hydrated gel layers, which subsequently recrystallize (silica-based bioactive glasses) or directly recrystallizes into bone-like constituents, based on hydroxyapatite-like minerals ($Ca_5(PO_4)_3OH$) (HAp).

Bioactive properties of certain glass compositions have been proposed since Larry Hench discovered the signature 45S5 Bioglass©[1], proposing that ionic products of glass dissolution could increase healing rates inside the human body[5]. The main disadvantage of the 45S5 Bioglass© is its silica matrix. Although soluble to some extent, these glasses endure the corrosive environments for periods longer than 30 days [6, 7]. The dissolution rate has been successfully reduced by adjusting the composition and the shape of the resulting material (e.g. fibers, microspheres[8]). Modified bioactive silicate glasses (13-93, 45S5) inevitably led to conclusions that not only silicate matrix, but also borate or phosphate glass networks produce hydroxyapatite-like material under corrosive conditions of simulated bodily environments[9-11].

This contribution proposes a novel bioactive glass composition, originating from a boron-containing alternatives to 45S5 Bioglass, specifically 13-93 glass. The new glass is characterised by its BPS (boro-phospho-silicate) matrix. The contribution also summarises the results of its preliminary chemical analysis after melt-quenching synthesis and the process of optimization of the melting process in order to prepare the glass of desired composition.

In the early stages of experiments, two samples of boron-containing glass have been prepared: 13-93B1 borosilicate glass ($34SiO_2$ $19B_2O_3$ $20CaO$ $12K_2O$ $5MgO$ $6Na_2O$ $4P_2O_5$ $_{wt\%}$) and 13-93B3 borate glass

($53B_2O_3$ 20CaO $12K_2O$ 5MgO $6Na_2O$ $4P_2O_5$ $_{wt\%}$). These boron-containing glasses were compared to the original Hench's silicate bioactive glass 45S5 ($45SiO_2$ 24.5CaO $24.5Na_2O$ $6P_2O_5$ $_{wt\%}$). In the second run, two potentially bioactive glass compositions were calculated and subsequently synthesized by melt-quenching route, namely BPS1 ($21B_2O_3$ 11CaO $8K_2O$ 4MgO $5Na_2O$ $16P_2O_5$ $_{wt\%}$) and BPS 2 ($18B_2O_3$ 20CaO $6K_2O$ 6MgO $6Na_2O$ $4P_2O_5$ $_{wt\%}$). Conventional melt-quenching method (High-temperature furnace Classic 0718E) was utilized to melt the glasses at 1100°C, 1200°C and 1300°C (13-93B1, 13-93B3, BPS series, respectively.) Bulk glasses were pulverized and sieved to 25µm particle size fraction for further use.

Novel glass BPS 1 was proposed to be more similar to HAp in terms of Ca/P ratio, but the melting experiment proved that high P content leads to rapid crystallization of calcium and potassium phosphate from the glass melt, thus producing a borosilicate glass with crystalline phosphate phase, i.e. a glass-ceramic material.

The composition BPS 2 was prepared in glassy form, as verified by X-ray diffraction (Panalytical Empyrean, CuKα radiation, operated at 45 kV and 40 mA in the 2θ range 10 - 80°) TG and DSC (Netzsch STA 449 F1) analysis was used to determine the glass transition temperature, T_g, and melting point of all prepared glasses.

Density of the prepared glasses was determined by helium pycnometry (Quantachrome Ultrapyc 1200e). Determination of glass density is vital information for corrosion assays, with borosilicate glass densities resulting in 2.4 g cm^{-3}.

Chemical analysis of listed materials was performed in cooperation with University of Technology, Brno, and Masaryk University, Brno. Quantification of elemental content was performed by inductively coupled plasma optical emission spectrometry (ICP-OES Thermo iCap 6500 duo). With highly linear calibration ($i^2 = 0.9999_9$), accurate results were achieved in 3 sample runs for each sample (see below)

The future task is to perform static corrosion test in deionized water at 37 °C with subsequent analysis of the dissolution products, with following analysis of pH change during the dissolution and ICP analysis of the corrosion environment (deionised water)

Table 1 BPS glass ICP-OES analysis result summary

		SiO_2	Na_2O	P_2O_5	CaO	B_2O_3	K_2O
λ(nm)	λ(nm)	288.1	588.9	213.6	422.6	249.6	479.9
BPS1	*wt%*	*35*	*5*	*14*	*11*	*21*	*6*
	res.	**35.2 ± 1.0**	**5.60 ± 0.19**	**16.14 ± 0.65**	**11.27 ± 0.48**	**20.36 ± 0.79**	**5.99 ± 0.39**
BPS2	*wt%*	*40*	*6*	*4*	*20*	*18*	*6*
	res.	**41.19 ± 0.65**	**6.45 ± 0.29**	**3.95 ± 0.14**	**20.49 ± 0.70**	**17.73 ± 0.70**	**6.10 ± 0.45**

Keywords: bioactive glass, silicate glass, borate glass, ICP-OES, quantification, characterization, corrosion

Acknowledgment:

This paper is a part of dissemination activities of project FunGlass.
This project has received funding from the European Union's Horizon 2020 research and innovation programme under grant agreement No 739566.

References:

1. L. L. Hench, I. D. Xynos and J. M. Polak, *Journal of Biomaterials Science-Polymer Edition*, 2004, **15**, 543-562.
2. L. L. Hench, *Journal of Materials Science-Materials in Medicine*, 2006, **17**, 967-978.
3. A. Jiřička, Ph.D. Dissertation thesis, University of chemical technology, 2002.
4. A. Helebrant, *Ceramics-Silikaty*, 1997, **41**, 147-151.
5. J. R. Jones, D. S. Brauer, L. Hupa and D. C. Greenspan, *International Journal of Applied Glass Science*, 2016, **7**, 423-434.
6. Q. A. Fu, M. N. Rahaman, H. L. Fu and X. Liu, *Journal of Biomedical Materials Research Part A*, 2010, **95A**, 164-171.
7. Q. A. Fu, M. N. Rahaman, B. S. Bal, L. F. Bonewald, K. Kuroki and R. F. Brown, *Journal of Biomedical Materials Research Part A*, 2010, **95A**, 172-179.
8. D. E. Day, J. E. White, R. F. Brown and K. D. McMenamin, *Glass Technology*, 2003, **44**, 75-81.
9. P. Balasubramanian, A. Grunewald, R. Detsch, L. Hupa, B. Jokic, F. Tallia, A. K. Solanki, J. R. Jones and A. R. Boccaccini, *International Journal of Applied Glass Science*, 2016, **7**, 206-215.
10. P. Balasubramanian, T. Buttner, V. M. Pacheco and A. R. Boccaccini, *Journal of the European Ceramic Society*, 2018, **38**, 855-869.
11. J. S. Fernandes, P. Gentile, A. Crawford, R. A. Pires, P. V. Hatton and R. L. Reis, *Tissue Engineering Part A*, 2017, **23**, 1331-1342.

Mesoporous Bioactive Glass – Part 1: Processing and Application

Fatih Kurtuldu[1], Dušan Galusek[2] and Aldo R. Boccaccini[3]

[1] Department of Biomaterials, FunGlass, Alexander Dubcek University in Trencin, Slovakia
(E-mail: fatih.kurtuldu@tnuni.sk)
[2] FunGlass, Alexander Dubcek University in Trencin, Slovakia
[3]Institute of Biomaterials, University of Erlangen-Nuremberg, Germany

ABSTRACT

According to the IUPAC definition, porous materials are divided into three classes: microporous (<2 nm), mesoporous (2–50 nm) and macroporous (>50 nm) [1]. Ordered mesoporous silica was first discovered in 1992 [2], and proposed as a drug delivery system in 2001 [3]. Since then silica-based glass microspheres, such as MCM-41, SBA-15 or MCM-48 type ordered mesoporous glass materials have been considered as an ideal material for incorporation of drugs, genes and other therapeutic agent carriers and control release systems. Mesoporous bioactive glasses can be prepared by sol-gel method, which is a wet-chemistry process for producing materials from building blocks such as the silicate tetrahedra, structural directive agents and metallic ions. This process mainly involves hydrolysis and condensation of precursors, drying, and stabilization. By controlling the processing parameters, the properties of the reaction product, such as its morphology and chemical and phase composition can be readily controlled. For the sol-gel synthesis of bioactive glasses, tetraethyl orthosilicate (TEOS) is the most widely used silicate precursor, while water and/or ethanol are used as solvents. The sol-gel process can take place under acidic or basic conditions, affecting the properties of the resulting materials: a simple changing of the pH of the solvent yields bioactive glasses with different morphology. In a typical sol-gel process used for preparation of bioactive glass nanoparticles, TEOS firstly undergoes hydrolysis and condensation in the presence of catalysts and structural directive agent to form SiO_2 nanoparticles. Metal ion precursors can be added during the hydrolysis and condensation of TEOS or after the formation of SiO_2 nanoparticles. The resulting nanoparticles are then dried and calcined.

In this preliminary study microemulsion sol-gel method was used for the preparation of mesoporous bioactive glass particles with spherical shape, monodispersed size and low degree of agglomeration. Microemulsions are thermodynamically stable, isotropic liquid mixtures of oil phase, aqueous phase and surfactants. In contrast to the formation of conventional emulsions usually requiring shear effects, microemulsions can form by simply mixing the components, which are then stabilized by the presence of surfactants [4], [5]. The schematic of the process of preparation of mesoporous glass nanoparticles via microemulsion method is shown in the Figure 1.

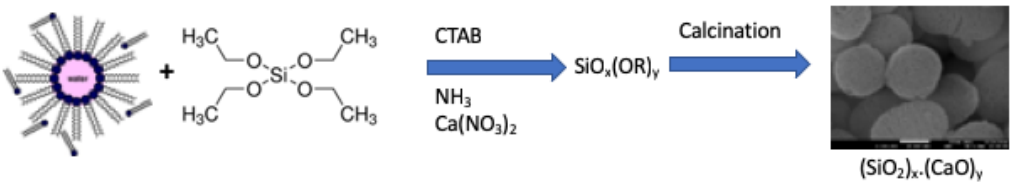

Figure 1 Preparation of Mesoporous Bioactive Glass Nanoparticles

In the present work, 2.8 g cetyltrimethylammonium bromide (CTAB soft template) was dissolved in 132 ml of water under continuous stirring for 15 min. Then, 40 ml of ethyl acetate was poured into the above solution. Aqueous solution of ammonium hydroxide (28%) and 14.4 ml of tetraethyl orthosilicate (TEOS) were then

added into the solution under continuous stirring. Finally, 10.15 g of calcium nitrate tetrahydrate was added, followed by magnetic stirring for 30 min. The solution was allowed to react for 4 h. After that, the suspension was filtrated and washed with deionized water and ethanol to remove unreacted precursors and remaining salts. The precipitates were dried in an oven at 40 °C overnight, followed by calcination at 650 °C (heating rate 1 °C/min) for 3 h. Fig. 2 shows the SEM micrographs of nanoparticles obtained by the experiment.

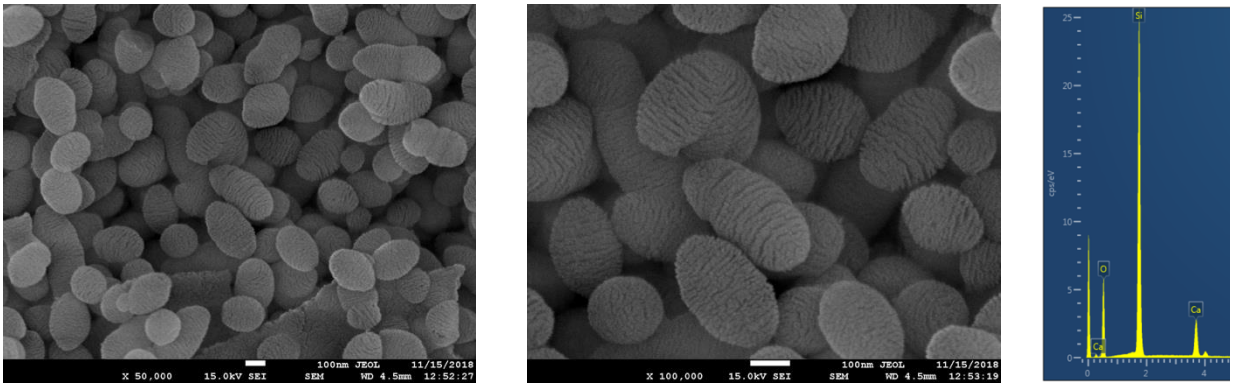

Figure 2 SEM images and EDX results of Mesoporous Bioactive Glasses produced by Micro-Emulsion Sol-Gel method.

Both silica and bioglass particles with pineal shape, and with the mean equivalent diameter of 150 nm were prepared during the experiment. The particles do not form agglomerates. The EDX results confirm that the glass nanoparticles contain 5-7 Atomic % Ca. The high resolution SEM micrographs revealed fine surface structure of the nanoparticles indicating their lamelar mesoporous structure. However, for unambiguous confirmation specific surface area measurements and TEM analysis are required.

Keywords: Drug delivery, Mesoporous Bioactive Glass, Nanoparticles

Acknowledgment:

This paper is a part of dissemination activities of project FunGlass.
This project has received funding from the European Union´s Horizon 2020 research and innovation program under grant agreement No 739566.

References:

[1] K. S. W. Sing, "Reporting physisorption data for gas/solid systems with special reference to the determination of surface area and porosity (Recommendations 1984)," *Pure Appl. Chem.*, vol. 57, no. 4, pp. 603–619, 1985.

[2] C. T. Kresge, M. E. Leonowicz, W. J. Roth, J. C. Vartuli, and J. S. Beck, "Ordered mesoporous molecular sieves synthesized by a liquid-crystal template mechanism," *Nature*, vol. 359, no. 6397, pp. 710–712, 1992.

[3] M. Vallet-Regi, A. Rámila, R. P. Del Real, and J. Pérez-Pariente, "A new property of MCM-41: Drug delivery system," *Chem. Mater.*, vol. 13, no. 2, pp. 308–311, 2001.

[4] M. A. Malik, M. Y. Wani, and M. A. Hashim, "Microemulsion method: A novel route to synthesize organic and inorganic nanomaterials. 1st Nano Update," *Arab. J. Chem.*, vol. 5, no. 4, pp. 397–417, 2012.

[5] K. Zheng and A. R. Boccaccini, "Sol-gel processing of bioactive glass nanoparticles: A review," *Adv. Colloid Interface Sci.*, vol. 249, pp. 363–373, 2017.

Mesoporous bioactive glasses – Part II: Biological response

Z. Neščáková, Liliana Liverani[2], Dušan Galusek[1], Aldo R. Boccaccini[2]

[1] FunGlass - Centre for Functional and Surface Functionalized Glass, Alexander Dubček University of Trenčín
(E-mail: zuzana.nescakova@tnuni.sk)
[2] Institute of Biomaterials, Department of Materials Science and Engineering, University of Erlangen-Nuremberg

ABSTRACT

Preclinical studies of bioactive glasses (BG) are first carried out in cell culture models (for this purpose primary culture or cell lines can be used). The cell culture model is a convenient way of screening the effectiveness of a BGs formulation. The cell culture models represent a major tool for the investigation of the normal physiology of the cells and possible toxic interaction between materials and biological system (1). The main advantage of using cell culture is consistency, reproducibility and shorter duration time of experiments. The cytotoxicity of a proposed material to a specific cell type can be studied either by directly seeding the cells on the surface of the material or by indirect evaluation by exposing the cells to the extraction fluid (2, 3).

In this work three different cell lines were used. Namely the MG-63 (human osteosarcoma cell line), MEFs (mouse embryonic fibroblasts cells) and ST-2 (mouse bone marrow stromal cell line) in the indirect elution test and indirect test in tissue cell culture inserts. Cytotoxicity of SiO_2-CaO and SiO_2-CaO-ZnO bioactive mesoporous glasses (MBGs) has been evaluated. Selection of cell types was based on the specific applications of MBGs. Human osteosarcoma cell lines could be a suitable model for orthopaedic implant materials. Mouse fibroblasts can be used for determining the cytotoxic potential of wound dressing material. Because of pluripotency of the stromal cell lines, they could be used as a model in both mentioned applications.

In the elution test method, extracts were obtained by placing the test materials in separate cell culture media incubated in standard conditions (24 h, 37°C). The obtained fluid extract was applied to a cultured-cell monolayer and jointly incubated for 2 days. In another indirect approach, the cells are in indirect contact with the material, but they are in the constant contact with released ions from the investigated material. Cells were located in the cell culture inserts, which represents a barrier between the cells and cell culture medium with the immersed material. The viability of the cells was obtained in 1 and 3 days (Fig.2).

To determine the viability of the cells in the contact with material was used WST-8 method. WST-8-(2-(2-methoxy-4-nitrophenyl)-3-(4-nitrophenyl)-5-(2,4-disulfophenyl)-2H-tetrazolium is bioreduced by cellular dehydrogenases to an orange formazan product. The amount of formazan produced is directly proportional to the number of living cells.

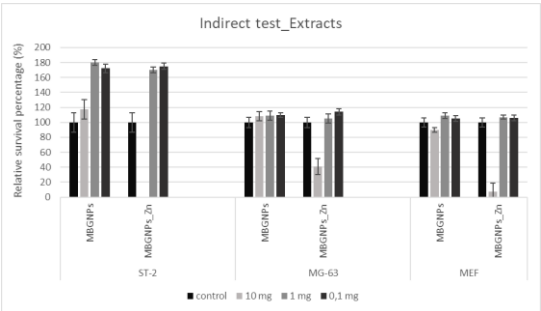

Fig. 1: Cytotoxicity testing – indirect elution test method. Influence of MBGNPs and MBGNPS_Zn powder extracts (10 mg/mL, 1 mg/mL, 0.1 mg/mL) on the viability of ST-2, MG-63 and MEF cells.

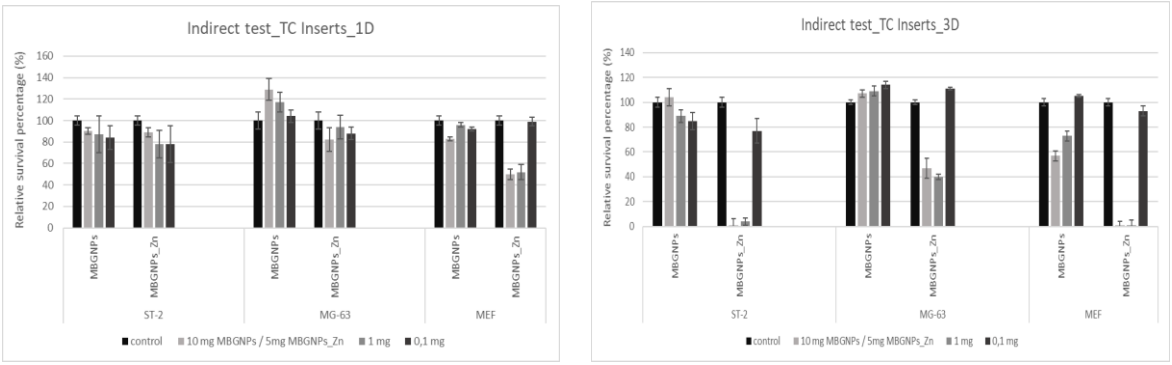

Fig. 2: Cytotoxicity testing – indirect method with use cell tissue culture inserts. Investigation of indirect influence of constantly releasing ions from MBGNPs and MBGNPS_Zn powder on the viability of ST-2, MG-63 and MEF cells after 1 day and 3 days of culture.

In the cytotoxicity testing, a negative result indicates that an MBGNPs material is free of harmful extracts for all tested concentrations with standard elution testing method and with the other approach which implies the use of tissue cell culture inserts (Fig. 1, Fig. 2). The cell viability of about 90 % characterizes a great biocompatibility potential of the MBGNPs. On the other hand, a positive elution cytotoxicity test result of MBGNPs_Zn (10 mg/mL), was an early warning sign, that a material contains extractable substances that could be of clinical importance (Fig. 1). Based on this fact MBGNPs_Zn undergone further investigation, titration in the elution test method, by means of which 5mg/mL concentration of the powder was determined as nontoxic for all tested cell lines (data not shown). Further cytotoxicity tests with seeded cells in cell tissue culture inserts on MBGNPs_Zn (5mg/mL) powder in constant contact with the cells, demonstrated that MBGNPs_Zn stays nontoxic for all cell lines after 1 day. However, the relative survival percentage of all tested cell lines was lower than 50 %, after 3 days, which indicate the cytotoxic effect of the material (Fig. 2).

In conclusion, cytotoxicity assay is a good first step toward ensuring the biocompatibility of proposed biomaterial. The material showed a variable cytotoxic potential which was related to the cell type. Obtained results confirmed the cell-line dependent sensitivity and support the necessity of the combination of at least two evaluation methods for *in vitro* cytotoxicity test.

Keywords: biomaterials, cytotoxicity, cell lines, indirect methods

Acknowledgement:

This paper is a part of dissemination activities of project FunGlass.
This project has received funding from the European Union´s Horizon 2020 research and innovation programme under grant agreement No 739566.

References:

1. Thrivikraman G., Madras G., Basu B. In vitro/In vivo assessment and mechanisms of toxicity of bioceramics materials and its wear particulates, *RSC Adv.*, 2014, 4, 12763-12781.
2. Wallin R.F., Arscott E.F., A Practical Guide to ISO 10993-5: Cytotoxicity, *Medical Device and Diagnostic Industry*, 1998, 4.
3. ISO DOCUMENT 10993-5. Biological evaluation of medical devices, Part 5, Tests for cytotoxicity: in vitro methods, 1992.

A traditional technique for obtaining 3D bioactive glass scaffolds with bone like structure

Susanta Sengupta[1]*, Martin Michalek[1], Dušan Galusek[1], Aldo R. Boccaccini[2]

[1]*Centre for Functional and Surface Functionalized Glass, Alexander Dubcek University in Trencin*
[2]*Institute of Biomaterials, Department of Materials Science and Engineering, University of Erlangen-Nuremberg, Erlangen, Germany*

Bone related problems are not a new issue in human life but they continue to rise with spreading of degenerative bone diseases in modern society. Synthetic biomaterials likebioactive glasses have a great impact in the field of orthopaedics and dentistry. Hench firstdiscovered the ability of glass materials to create a bond with bones. Bioactive glasses[1] (silicate and borate based) like 45S5, 13-93, 13-93B3, 160S and 58S have the ability to form bone minerals, like hydroxycarobonated apatite (HCA), after immersion in simulated body fluid (SBF). Dissolution of ions (B, Cu, Zn, Mg, Co, Sr, Ca) from glass into the body fluid and increasing concentration of some particular ionscontribute to the formation of the HCA layer. Moreoverthe release of such ions leads to the biological activity of bioactive glasses which act as a vehicle for the delivery of biologically active ions. Thus, current research oftenfocuses on incorporation of such type of metal ions into bioactive glasses to enhance their bioactivity.Boron is one of the elements which plays a significant role in fast bone growth, i.e. it acts as a bone growth stimulating agent, being also an angiogenicagent[2] Boron modified 45S5 bioactive glass particles exhibit more pronounced bioactivity than the un-doped 45S5 glass. Also, scaffolds made from bioactive glasses show great promise for bone replacement and regeneration in bone tissue engineering approaches. There is a need for the development of synthetic scaffolds for the repair of large defects in load bearing bones such as long limb bones. A number of methods like solid freeform fabrication, solvent casting, freeze casting, robocasting and foam replication is used to fabricate three dimensional (3D) scaffolds. Factors like porosity and pore diameter in the porous 3D scaffolds play an important role in the mechanical strength and bioactivity of the scaffolds. However, the scaffolds prepared by various conventional methods often lack the desired combination of porosity and mechanical strength for bone repair and regeneration.

In our present research work we applied a conventional tape casting method[3]traditionally usedin the field of ceramic processingfor preparation of bioactive 3D scaffolds with highly interconnected porous microstructure.Firstly, we prepared the 13-93B3 bioactive glass with composition ($53B_2O_3$, $6Na_2O$, $12K_2O$, $5MgO$, $20CaO$, $4P_2O_5$) by melt quench method. Scaffolds were prepared inthe form of discs with the diameter of 10 mm using tape casting from organic suspension of glass particles. For this purpose the glass was ground and sieved to obtain glass powder with particle sizes ≤25µm. Poly-vinyl butyral (PVB) and PEG-300 were then added to ethanol suspension of the glass powder with 25 vol% solid loading. The glass tapes were prepared with the use of the laboratory tape caster (Pro-cast, Hed International, New Jersey, USA).The thickness of the green tape was adjusted by the height of the Doctor's blade gap in the range between 200 to 250 µm. The sintering behaviour of the tapes was examined by heating the tapes at different temperatures with different holding times. The tapes were heat treated at 550 ^{0}C, 575 ^{0}C and 600 ^{0}C without holding time and also with dwell time of 1h, 2h, 3h and 4h. With increasing the sintering temperature and holding time it was observed that tapes sintered at 575 ^{0}C for 1h sintered better (lower residual porosity) than tapes sintered at 550 ^{0}C with the same holding time. The tapes were completely sintered with no residual porosity at 600^{0}C with holding time of 1h. As completely sintered tapes are not useful as scaffolds for bone regeneration, the heat treatment profile of 550 ^{0}C with holding time 1h was selected for further

experiments. XRD results confirmed that crystalline phases wereformed during heat treatment in the temperature interval studied. This formation is crucial, as the formation of crystalline phases in scaffold materials can reduce their bioactivity but also increase the mechanical strength of the scaffold. The tapes were cut into circular discs and stacked (10 tapes) together using a hydraulic press at an applied pressure of 6 MPa. The stackswere heat treated using the heat treatment profile specified above.

In our future work PMMA microspheres with diameter ranging from 106 to 125 µm (Cospheric, USA)will be added to suspensions in order to prepare tapes with controlled porosity, which will be further used as building blocks for preparation of porous scaffolds. The bioactivity of these scaffolds will be tested *in vitro*, in the SBF according to Kokubo et. al.[4] Based upon the results of the *in vitro* analysis, *in vivo* studies are envisaged on selected scaffolds. The final objective is to evaluate the mechanical response and bioactivity of the scaffolds after implantation in the animal body.

References:

1) A. A. El-Rashidy, J. A. Roether, L. Harhaus, U. Kneser, A. R. Boccaccini, ***ActaBiomater*** 62 (2017) 1-28.
2) P. Balasubramanian, T. Buttner, V. M. Pacheco, A. R. Boccaccini, ***J. Eur. Cer. Soc.*** 38 (3), (2018) 855-869.
3) M. Jabbari, R. Bulatova, A.I.Y Tok, C.R.H. Bahl, E. Mitsoulis, J.H. Hattel, ***Mat. Sci. Eng-B*** 212 (2016) 39-61.
4) T. Kokubo, H. Takadama, ***Biomaterials*** 27 (2006) 2907-2915.

Keywords: Bioactive glass, 3D Scaffold, Bone regeneration, Tape casting, Pore

This abstract is a part of dissemination activities of project Fun Glass.
This project has received funding from the European Union´s Horizon 2020 Research and innovation programme under grant agreement No 739566

Incorporation of Fibrous/Particulate Bioglass in Soft Matrices for Soft Tissue Applications

Nurshen Mutlu[1], Dušan Galusek[2] and Aldo R. Boccaccini[3]

[1] Department of Biomaterials, FunGlass, Alexander Dubcek University, Trencin, Slovakia
(E-mail: nursen.mutlu@tnuni.sk)
[2] FunGlass, Alexander Dubcek University, Trencin, Slovakia
[3] Friedrich–Alexander University Erlangen–Nürnberg, Germany

ABSTRACT

Application of bioactive glasses in orthopedic and dental application, as well as bone tissue engineering gained a great interest in the last 50 years since its discovery by Hench et al. in 1971 [1]. Most frequently studied and well documented system for bone filling materials, dental application and bone implants are the bioglass compositions 455S (45% SiO_2, 24.5% Na_2O and CaO, 6% P_2O_5 by wt.) and 13-93 (53% SiO_2, 20% CaO, 12% K_2O, 6% Na_2O, 5% MgO, 4% P_2O_5). Recently boron containing glasses attracted attention for applications for beyond bone and teeth: soft tissue applications including wound healing are also studied. Bioactive borate glasses show 5 times faster biodegradation and better bioactivity. Unlike the 45S5 silicate bioactive glass, they transform to hydroxyapatite (HA) completely. This feature originates from less stable structure of boron containing glasses. The ions, such as B, Na and Ca, which release into surrounding area have been observed to contribute to regulation of the wound healing process [2], [3], [4].

To provide an optimum environment for creating new tissue, biomaterials have to allow transportation of nutrition and oxygen between cells and extracellular matrix. To achieve this, polymer matrices such as polylactic acid are widely used because of its low cost, low energy required during production process. They are also easily thermally processible, nontoxic for human body and possess Food and Drug Administration approval. However, the polymers by themselves are insufficient in providing required mechanical strength, chemical reactivity, biocompatibility and bioactivity to mimic natural tissue. Their mechanical properties must be improved and optimized, and additional bioactivity has to be provided by other components. Borate glasses are candidate for preparation of a composite material which could provide temporary support for creating new tissue formation [5].

In my future work, I will produce borate glass with Zn as a therapeutic ion via conventional glass melting process. Powder form of borate glass will act as a reinforcement component for composite materials. Thermally induced phase separation method (TIPS) will be used for scaffold preparation by providing convenient scaffold architecture including amount, size, and, shape of porosity, and freeze drying will be applied for removing the solvent from scaffold. After morphology and porosity analysis, mechanical properties will be measured. Phosphate buffered saline (PBS) solution will be prepared for biodegradation study, bioactivity test will be carried out with the use of a simulated body fluid (SBF), and evaluated by the change of the SBF chemical composition by ICP OES.

Keywords: Bioglass, soft matrice, soft tissue.

Acknowledgment:

This paper is a part of dissemination activities of project FunGlass.
This project has received funding from the European Union´s Horizon 2020 research and innovation program under grant agreement No 739566.

References:

[1] L. L. Hench, R. J. Splinter, W. C. Allen, and T. K. Greenlee, "Bonding mechanisms at the interface of ceramic prosthetic materials," *J. Biomed. Mater. Res.*, vol. 5, no. 6, pp. 117–141, 1971.

[2] P. Balasubramanian, T. Büttner, V. Miguez Pacheco, and A. R. Boccaccini, "Boron-containing bioactive glasses in bone and soft tissue engineering," *J. Eur. Ceram. Soc.*, vol. 38, no. 3, pp. 855–869, 2018.

[3] V. Miguez-Pacheco, L. L. Hench, and A. R. Boccaccini, "Bioactive glasses beyond bone and teeth: Emerging applications in contact with soft tissues," *Acta Biomater.*, vol. 13, pp. 1–15, 2015.

[4] J. Zhou *et al.*, "In vivo and in vitro studies of borate based glass micro-fibers for dermal repairing," *Mater. Sci. Eng. C*, vol. 60, pp. 437–445, 2016.

[5] L. Gritsch, G. Conoscenti, V. La Carrubba, P. Nooeaid, and A. R. Boccaccini, "Polylactide-based materials science strategies to improve tissue-material interface without the use of growth factors or other biological molecules," *Mater. Sci. Eng. C*, no. September, pp. 0–1, 2018.

Inline measurement of leachates from bioglass immersion tests

***Dagmar Galusková, Hana Kaňková, Dušan Galusek**

Centre for Functional and Surface Functionalized Glass,
Alexander Dubček University of Trenčín, Študentská 2, 91150 Trenčín, Slovakia
*corresponding author: dagmar.galuskova@tnuni.sk

The use of simulated body fluid (SBF) for bioactivity testing has exploded in bio community. The SB fluid was developed initially to evaluate surface structural changes of glass-ceramics used to manufacture artificial vertebrae, ileum, tooth roots, and bioactive material used to repair hard tissues such as artificial middle-ear bone and maxillofacial implants [1]. Variety of tests are performed with SBF solution including apatite-forming ability test, leaching or immersion tests. What do these tests have in common is evaluation of dissolved species, particularly ions transferred from immersed biomaterial into SBF solution [2]. The formation of apatite on a material dipped in SBF is proved on the basis of decrease of concentration of calcium and phosphate ions in the SBF. Except from Ca and P other elements can be present in solution depending on the chemical composition of biomaterial and kinetics of its dissolution. The bio-glass structure is composed from network formers: silicon, boron, phosphorus, as well as modifiers: alkali or alkaline earth elements. A variety of therapeutic ions e.g. Co, Cu, Sr, Zn or ions (Y, Ce) can be also incorporated into bioglass structure. Immersion tests reported in scientific literature usually rely on evaluation of the dissolution in only few time intervals, e.g 1, 3, 7 and 14 days, not taking into account the fact that the first hours of leaching often provide valuable information on leaching kinetics and represent the most important part of the dissolution curve. In this short communication, the experimental procedure for inline measurement of leachates from bioglass immersion tests is discussed and the limits of quantification for therapeutic ions in SBF solution are presented.

EXPERIMENTAL PART

For the *flow-through* test the thermostatic bath, corrosion cell, peristaltic pump and tubing were assembled and connected directly to the introduction system of the optical emission spectrometer (ICP OES, VARIAN MPX). Internal standard scandium (10 mg/L) was included in inline sampling in order to deal with non-spectral interferences. SBF buffer solution was prepared according to the protocol described by Kokubo and colleagues [2] at 37 °C and pH 7.4. Limit of detection for therapeutic ions together with silicon and boron, the elements not dissolved in SBF solution, was determined. Limit of quantification with precision calculated as RSD% was considered to be < 5%. Dissolution of the borosilicate glass prepared in FunGlass centre by Dr. Si Chen labelled as BG10B4Co was used for optimization of the experimental parameters of inline measurement of leachates. The pump rate and replicate time was considered and the following parameters were selected respectively: 10rpm (~0.7 mL/min) and 60 s. Inline tests were conducted with 500 mg of bioglass sample soaked in 10 mL volume cell, through which continuously flew fresh SBF solution at the temperature held constant at 37±1 °C. Concentration of Ca, P, B, Si and Co as function of time was directly monitored using ICPExpert software. The total amount of leached elements (*Q*) is determined by the following equation [3]:

$$Q_i^t = c_i \frac{F}{m} \Delta t + Q_i^{t-\Delta t} \qquad (1),$$

where c_i is concentration of particular leached element in time t, F is the flow rate. Values of the initial leaching rate may be evaluated from experimental time dependencies of Q_i.

RESULTS AND DISCUSSION

The reference SBF solution was scanned for 45 min period of time. Limits of quantification were calculated as 10x of the value of standard deviation from all recorded data (Table 1).

Table 1: *Limits of detection (LOD) and limits of quantification (LOQ) for selected elements in the simulated body fluid.*

element [nm]	B *249.772*	Co *228.615*	Cu *324.754*	Si *288.158*	Sr *216.596*	Sr *421.552*	Zn *202.548*
LOD	0.007	0.02	0.02	0.04	0.008	0.001	0.02
LOQ	**0.02**	**0.07**	**0.06**	**0.1**	**0.03**	**0.004**	**0.05**

The data from the flow through test of the Co-containing borosilicate bioglass 10B4Co were collected in the time interval of ~ 70 min. Chemical durability of selected bioglass was tested against SBF solution. Deionized water was used as the reference medium. Time dependence of released ions calculated according to equation (1) for deionized water and SBF solution is shown respectively, in the Fig. 1 and 2.

Fig. 1: *The total amount of leached elements from bioglass directly measured in deionized water.*

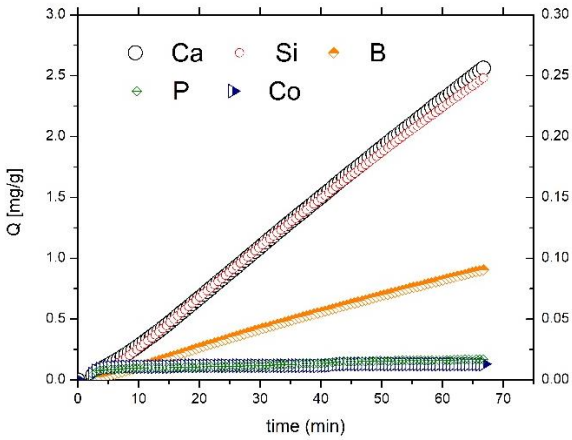

Fig. 2: *The total amount of leached elements from bioglass directly measured in SBF solution.*

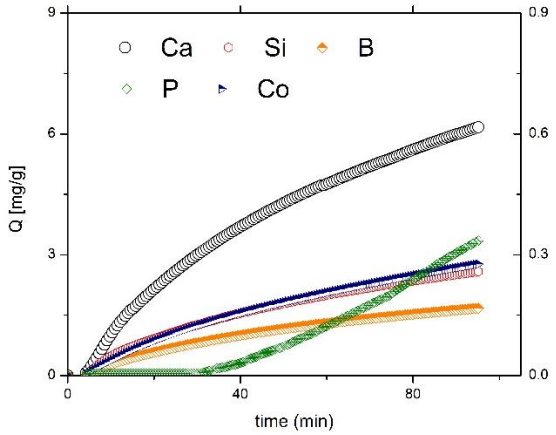

The lowest detectable leached amount 10 and 5 mg/L for Ca and P, respectively, which differentiate with 5% confidence from the content of calcium and phosphorus in SBF was included in the calculations. For deionized water the kinetic performance is linear (Fig. 1), while for SBF solution nonlinear time dependence of total leached amount for Ca, B and Si are plotted in Fig. 2. Discussion related to the rate of dissolution and characterization of kinetic curves is beyond the scope of this article.

CONCLUSIONS

Inline measurement of the concentration profile for the *flow-through tests* was optimized for studying dissolution curves of borosilicate bioglass. Time dependent dissolution curves were plotted in order to study chemical durability of bioglass in deionized water as well in simulated body fluid solution. Limits of quantification with precision of less than 5% (RSD) were determined for analysis of therapeutic ions in SBF.

Keywords: bioglass, kinetics, SBF

Acknowledgment:

This paper is a part of dissemination activities of project FunGlass. This project has received funding from the European Union´s Horizon 2020 research and innovation program under grant agreement No 739566.The financial support of this work by the grant VEGA 2/0026/17 is gratefully acknowledged.

References:

[1] Marques R.C., Loebenberg R., Almukainzi M. Simulated biological fluids with possible application in dissolution testing? Dissolution Technologies 18(3), 15–28 (2011)
[2] Kokubo T., Takadama H. How useful is SBF in predicting in vivo bone bioactivity? Biomaterials 27, 2907–15 (2006)
[3] Mišíková L., Galusková D., Corrosion of E-glass fibers, security factor of nuclear power plants, Ceramics-Silikáty 50 (2006)

Flame synthesis of binary aluminate glass microspheres

Jana Valúchová[1,2], Anna Prnová[1,2], Milan Parchovianský[2], Peter Švančárek[1,2], Dušan Galusek[1,2]

[1]Join Glass Centre of the IIC SAS, TnUAD, FChPT STU, Študentská 2, 911 50 Trenčín, Slovakia
(E-mail: jana.valuchova@tnuni.sk)
[2]FunGlass, A. Dubček University of Trenčín, Študentská 2, 911 50 Trenčín, Slovakia

ABSTRACT

The aim of this work is preparation and study of properties Al_2O_3-Y_2O_3 glass microspheres. For these glasses excellent mechanical and optical properties comparable to that of single crystal sapphire are expected. Because Al_2O_3 is not a typical glass-former, preparation of these glasses in bulk is very difficult due to high crystalization rates and high melting temperatures, and require therefore high temperatures and high cooling rates. Yttrium aluminate glasses with eutectic composition AY-E (76.8 mol. % Al_2O_3) were prepared in the form of glass microspheres by flame synthesis. The highly homogenous starting powders for flame synthesis were prepared by sol-gel (Pechini) method using corresponding nitrates as starting materials. The basic characterisation of prepared glass microparticles was carried out by XRD, OM and SEM. Two exothermic peaks with maxima at 942 and 1006°C were observed in DSC record. The high temperature X-ray powder diffraction measurements (HT XRD) were carried out in the temperature interval 750 -1450°C with the step of 5°C and the temperature dependence of phase composition was determined. The crystallisation of YAG (yttrium-aluminate garnet) phase was observed in relatively broad temperature interval 900-1200°C, with the steep increase of the YAG phase content between 900 and 950°C, followed by slower increase between 1100 and 1300 °C. The crystallisation of α-Al_2O_3 phase follows at temperatures > 1300°C. Preliminary experiments with hot-pressing of the microspheres have been carried out, and the results are reported.

Keywords: yttrium-aluminate glasses, YAG, SEM, DSC, HT XRD

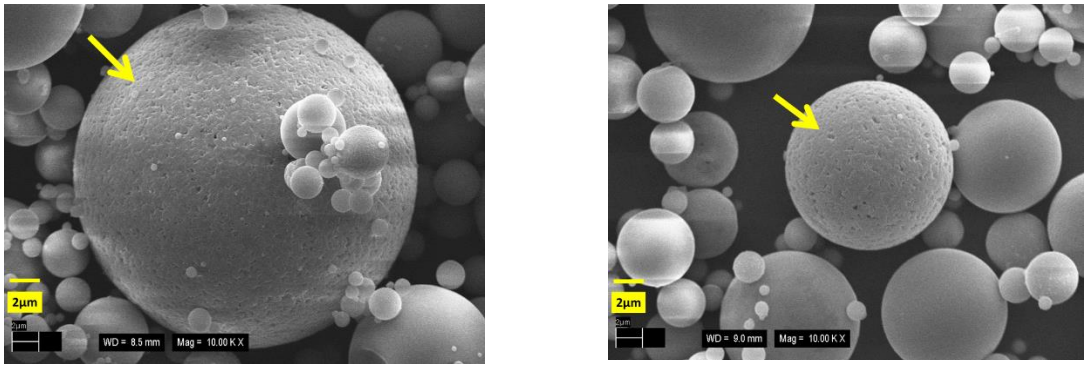

Fig.1 SEM micrographs of YA-E microspheres prepared by flame synthesis**.** The particles with morphological features (facets) suggesting their polycrystalline nature are marked by arrows.

Acknowledgment:

This paper is a part of dissemination activities of project FunGlass.
This project has received funding from the European Union´s Horizon 2020 research and innovation programme under grant agreement No 739566.
The financial support of this work by the projects APVV 0014-15, VEGA 1/0527/18, VEGA 2/0026/17 is gratefully acknowledged.

The temperature dependence of the impedance spectrum of the barium crystal glass

Katarína Faturíková[1], Marek Liška[2,3], Peter Viščor[4]
[1] Central Laboratories, FunGlass, Alexander Dubček University of Trenčín, Študentská 2, SK-911 50 Trenčín, Slovakia

[2] VILA – Joined Glass Centre of the IIC SAS, TnUAD, FChPT STU, Študentská 2, SK-911 50 Trenčín, Slovakia
[3] VILA, FunGlass, A. Dubcek University of Trenčín, Študentská 2, SK-911 50 Trenčín, Slovakia
[4] EIS Laboratory, Skjoldenaesvej 17, 4174 Jystrup, Denmark

ABSTRACT

Electrical impedance spectroscopy (EIS) technique is a non-destructive powerful technique for the characterization of the electrical behavior of material. This technique can be used as electrical characterization tool in materials research and development when studying defects, microstructure, surface chemistry, electrical conductivity and electrical permitivity for a wide range materials, including dielectrics and ionic conductors and to study various polarization processes as a function of applied external electric field. The technique involves the measurement of the sinusoidal component of the current flowing through the sample, resulting from the sinusoidal voltage, applied across two terminals of a sample [1, 2, 3].

A comprehensive Electrical Impedance Spectroscopy study of the electrical response of barium crystal glass has been undertaken in order to determine various electrically active physical processes taking place in this system. The temperature dependence of the impedance spectra of the barium crystal glass was studied in an interval from 50°C to 400°C with step 50°C, in the frequency range from 1mHz to 1 MHz. Samples with thickness 0,7mm, 1mm, 1,7mm and 2,5mm were studied.

Investigations of the relaxation processes in dielectric materials are usually restricted to an analysis of the frequency dependences of the real (ε') and imaginary (ε") parts of the complex dielectric permittivity $\varepsilon = \varepsilon' - i\varepsilon''$ [4, 5].

In this contribution the temperature and thickness dependence of the dc conductivity and the distribution of relaxation times of dielectric relaxation will be presented and shortly discussed.

Keywords: electrical impedance spectroscopy, dielectric properties, barium glass, distribution of relaxation times

References:

[1] NITSCH, K.: Microelectronic materials and structures characterization by impedance spectroscopy. Microelectronics reliability, vol. 51, 2011. p. 1213-1218.
[2] MICKA, K.: Introduction into the theory of impedance measurements. Praha: VŠCHT, 2001, ISBN 80-7080-228-6.
[3] BARSOUKOV, E., MACDONALD, J.R.: Impedance spectroscopy: Theory, Experiment and Applications, New Jersey: Wiley, 2005. ISBN 0-471-64749-7.
[4] Turik A. V., Rodinin M. Yu. Dielectric Losses in Materials with Limited Range of Relaxation Times. Technical Physics Letters, 2010; 36; 16–18.
[5] Constantino Grosse. A program for the fitting of Debye, Cole–Cole, Cole–Davidson, and Havriliak–Negami dispersions to dielectric data. Journal of Colloid and Interface Science, 2014; 419; 102–106.

Acknowledgment:

This paper is a part of dissemination activities of project FunGlass.
This project has received funding from the European Union´s Horizon 2020 research and innovation programme under grant agreement No 739566.
This work was supported by The Slovak Grant Agency for Science under grant No. VEGA 2/0088/16, VEGA 1/0064/18 and APVV 0487-11.

Some Peculiarities of the Isoconversional Methods

Peter Šimon, Tibor Dubaj, Zuzana Cibulková and Anna Vykydalová

Institute of Physical Chemistry and Chemical Physics, Faculty of Chemical and Food Technology, Slovak University of Technology, Radlinského 9, SK-812 37 Bratislava, Slovakia (E-mail: peter.simon@stuba.sk)

ABSTRACT

Solid state processes are extensively studied by thermoanalytical methods. Mechanisms of these processes are very often unknown or too complicated to be characterised by a simple kinetic model. They tend to occur in multiple steps that have different rates. To describe their kinetics, isoconversional methods are often used.

The principal idea of isoconversional methods is very simple, there are only two basic assumptions [1]:
(i) Rate of the processes in condensed state is generally a function of temperature and conversion:

$$\frac{\mathrm{d}\alpha}{\mathrm{d}t} = \Phi(T,\alpha) \qquad (1)$$

The isoconversional methods employ the assumption that the function Φ in Eq. (1) can be expressed as a product of two functions independent of each other, the first one, $k(T)$, depending solely on temperature T and the other one, $f(\alpha)$, depending solely on the conversion of the process, α:

$$\Phi(T,\alpha) = k(T)\mathrm{f}(\alpha) \qquad (2)$$

Combining Eqs.(1) and (2), the rate of the process can then be formally described by a single-step rate equation [2] even though the kinetics of a complex process should be described by a set of kinetic equations. Eq.(3) is called the general/generalized kinetic equation. It is a mathematical tool enabling to described the kinetics of a complex process in a simple and feasible manner

$$\frac{\mathrm{d}\alpha}{\mathrm{d}t} = k(T)\mathrm{f}(\alpha) \qquad (3)$$

(ii) The kinetic parameters are obtained from a set of kinetic runs from the dependences of time *vs*. temperature (for isothermal measurements), temperature vs. heating rate (for integral and incremental methods with linear heating rate) or from reaction rate vs. temperature (for the differential Friedman method). The evaluation is carried out at the fixed conversion α [1].
The isoconversional methods can be roughly divided into three groups, i.e. the integral, incremental and differential methods [1]. The most popular and most employed are the integral isoconversional methods. Very often, as a result of kinetic analysis, the kinetic parameters obtained appear to depend on the conversion. In this case, the kinetic analysis is mathematically incorrect and extrapolated approximations may lead to nonsensical dependences, such as shown in [3] (see Fig.1). In such a case, application of the incremental methods is advisable [4].

Another quite strange thing with the isoconversional methods is that the experimental kinetic data can be described equivalently by several temperature functions, not only by the Arrhenius function (see Fig.2). First, who realized that fact and justified it, was Laidler [5]. For the evaluation of kinetic data and futher application of the kinetic parameters obtained, the Bethelot-Hood temperature function appeared to be most suitable [6].

$$k(T) = A_{\mathrm{k}}\mathrm{e}^{DT} \qquad (4)$$

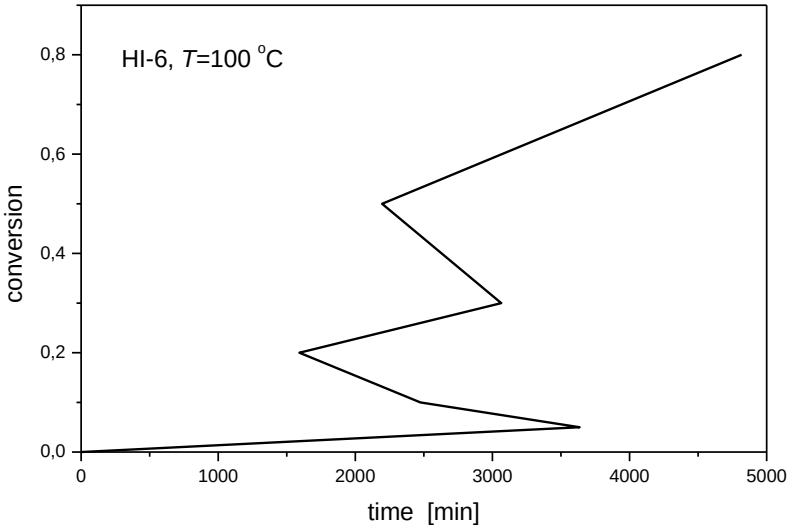

Fig.1: Dependence of conversion on time calculated using the kinetic parameters from thermogravimetric measurements with linear heating foir the drug HI-6.

Keywords: extrapolation, isoconversional, kinetics, solid state, thermal analysis, temperature function.

Acknowledgment:

This paper is a part of dissemination activities of project FunGlass.
This project has received funding from the European Union´s Horizon 2020 research and innovation programme under grant agreement No 739566.
Financial support from the Slovak Research and Development Agency (APVV-15-0124) is also gratefully acknowledged.

References:

[1] P.Šimon, J.Therm.Anal.Calorim. 76 (2004) 123-132: Isoconversional methods: Fundamentals, meaning and application.
[2] P.Šimon, J.Therm.Anal.Calorim. 82 (2005) 651-657: Considerations on the single-step kinetics approximation.

[3] P.Šimon, P.Thomas, T.Dubaj, Z.Cibulková, A.Peller, M.Veverka, J Therm Anal Calorim 115 (2014) 853–859: The mathematical incorrectness of the integral isoconversional methods in case of variable activation energy and the consequences.

[4] T.Dubaj, Z.Cibulková, P.Šimon, J. Comput.Chemistry 36 (2015) 392–398: An incremental isoconversional method for kinetic analysis based on the orthogonal distance regression.

[5] P.Šimon, T.Dubaj, Z.Cibulková, J Therm Anal Calorim 120 (2015) 231–238: Equivalence of the Arrhenius and ,non-Arrhenian temperature functions in the temperature range of measurement.

[6] P.Šimon, D.Hynek, M.Malíková, Z.Cibulková, J Therm Anal Calorim. 93 (2008) 817–821: Extrapolation of accelerated thermooxidative tests to lower temperatures applying non-Arrhenius temperature functions.